Seismo-electromagnetics: Modelling and Observation

Hong-Jia Chen

24 March 2020 @ NCU, Taiwan

Education:

2008-2010: Master Degree of Earth Science, Department of Earth Sciences, National Central University.

2013-2018: PhD Degree of Earth Science, Department of Earth Sciences, National Central University.

Experience:

2010-2013: Assistant Researcher, Research & Development Alternative Military Service, Seismological Center of Central Weather Bureau.

2016-2017: Guest PhD Student, ETH Zurich, Switzerland (MOST project).

2019-2020: Postdoc Researcher, Department of Earth Sciences, Graduate School of Science, Chiba University (MOST project).

CHIBA UNIVERSITY

ETH zürich

國立中央大學

References

- H.-J. Chen, Z.-K. Ye, C.-Y. Chiu, L. Telesca, C.-C. Chen, and W.-L. Chang (2020). Self-potential ambient noise and spectral relationship with urbanization, seismicity, and strain rate revealed via the Taiwan Geoelectric Monitoring Network. *J. Geophys. Res. Solid Earth*.
- H.-J. Chen, Chen, C.-C., Ouillon, G., and Sornette, D. (Accepted). Coupled mechano-electrokinetic Burridge-Knopoff model of fault sliding events and transient geoelectric signals. *EPJ Special Topics*.
- H.-J. Chen, Chen, C.-C., Ouillon, G., and Sornette, D. (Accepted). A paradigm for developing earthquake probability forecasts based on geoelectric data. *EPJ Special Topics*.
- H.-J. Chen, K. Hattori, R. Takahira, C.-C. Chen (Preparing). Pre-earthquake early-warning signals of ULF geoelectric data and their forecasting probability: A case in Kakioka, Japan. *Geosciences*.

What is seismo-electromagnetics?

- A coupling between mechanics and electromagnetics in the crust
- Various electromagnetic phenomena generated by tectonic forces acting on the earth's crust, associated with seismic activity
- Final goal: to provide a basis for short-term earthquake forecasts

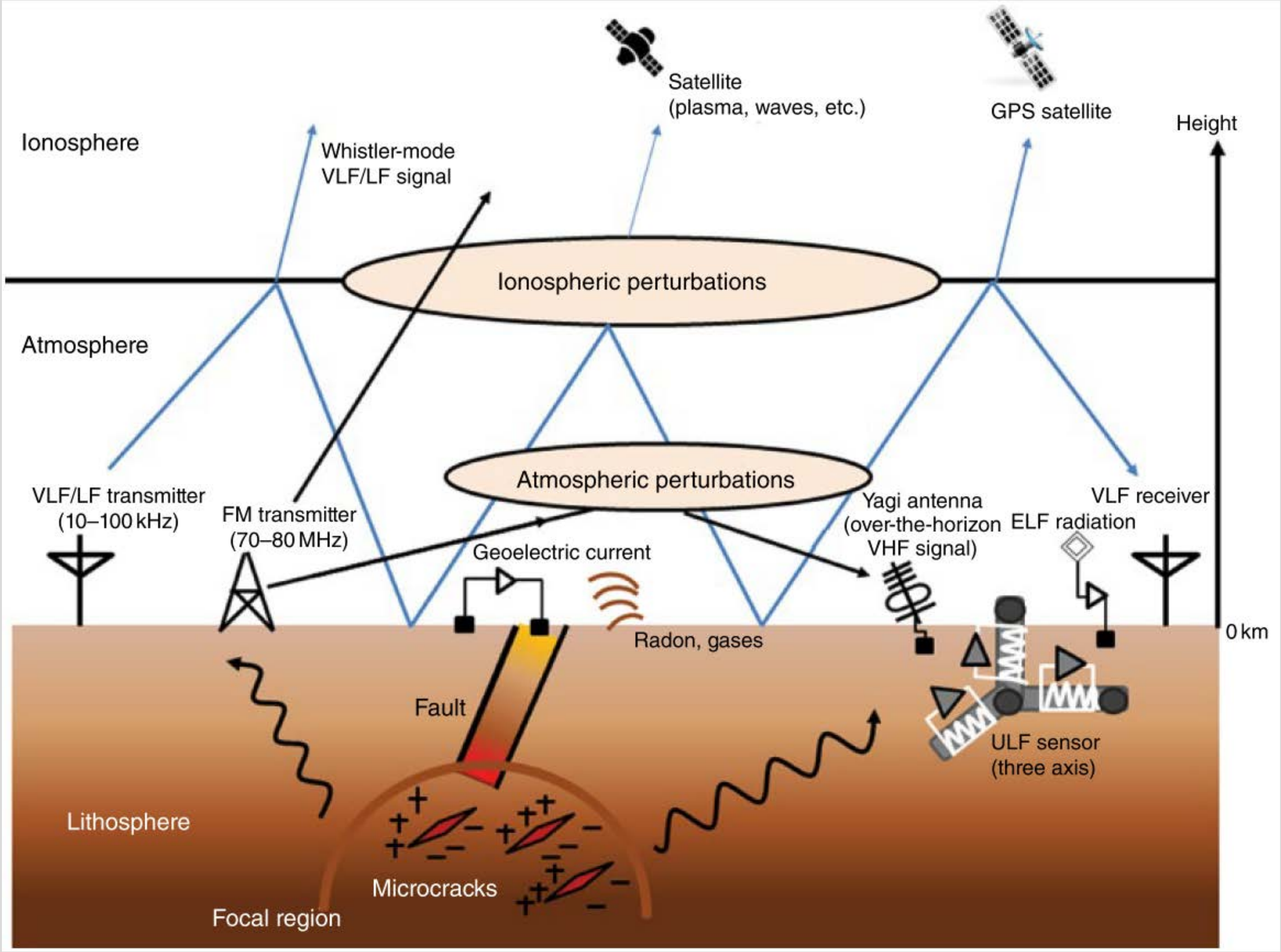

[Hayakawa, 2018]

Literature Survey

Seismo-electromagnetics

Lab Experiments

Field Observations

Model Simulations

Case study

Power spectral analysis

$P(f) = \alpha f^{-\beta}$

Scarcity

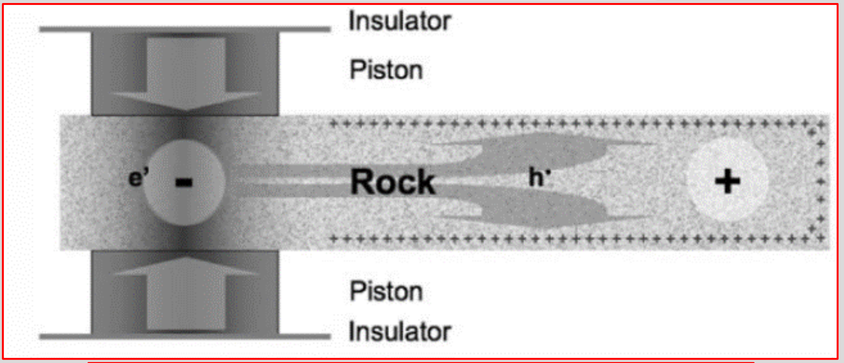

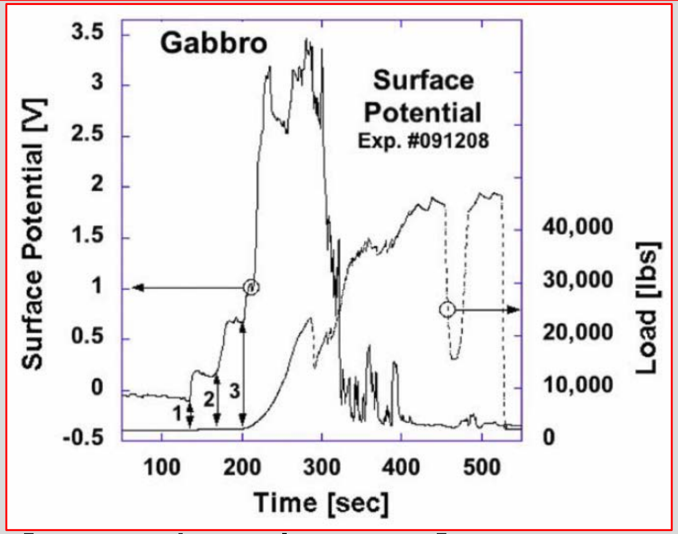

[Freund et al., 2009]

Possible mechanism:

Peroxy-defect theory

Piezoelectricity

Electrokinetics

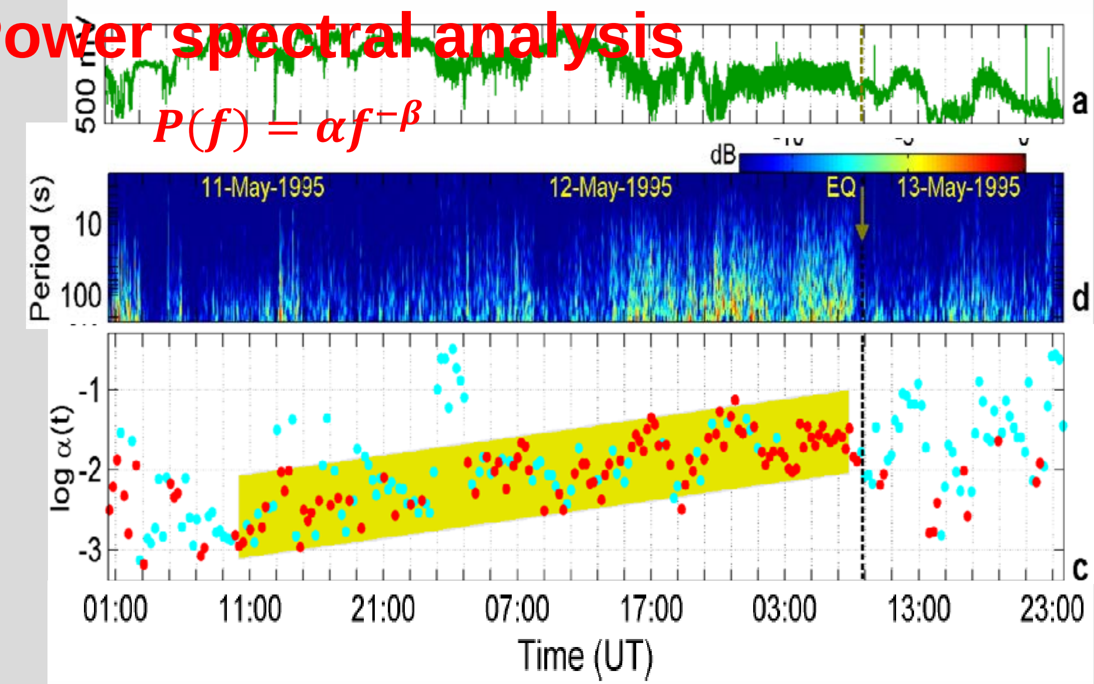

[Eftaxias et al., 2003]

Chen-Ouillon-Sornette (COS) model

Seismo-electric model:

- ➢ Crustal mechanics: Burridge-Knopoff spring-block model
- ➢ Crustal electricity: ???
- ➢ Rock-fracturing experiment: positive relationship between stress & voltage

Mechanical component

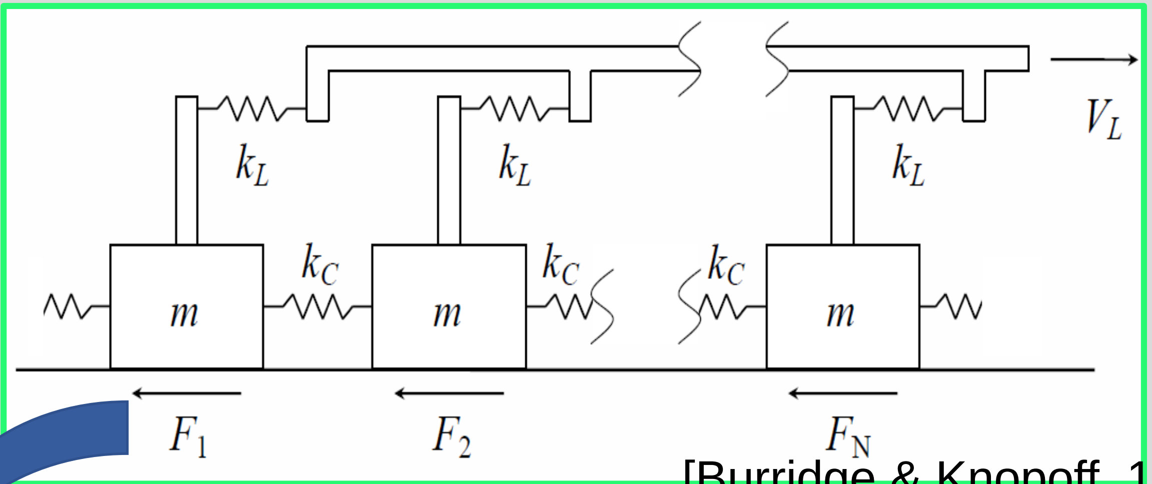

[Burridge & Knopoff, 1967]

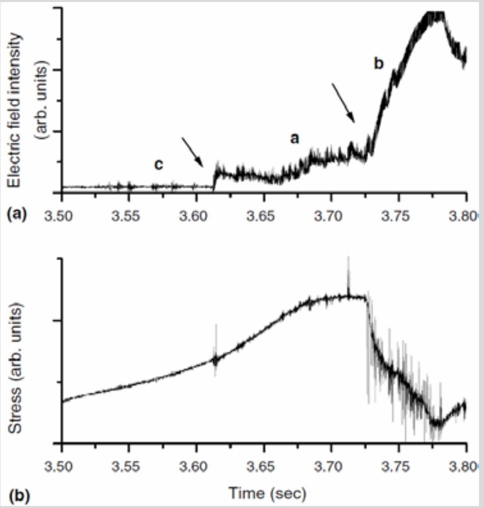

[Mavromatou et al., 2004]

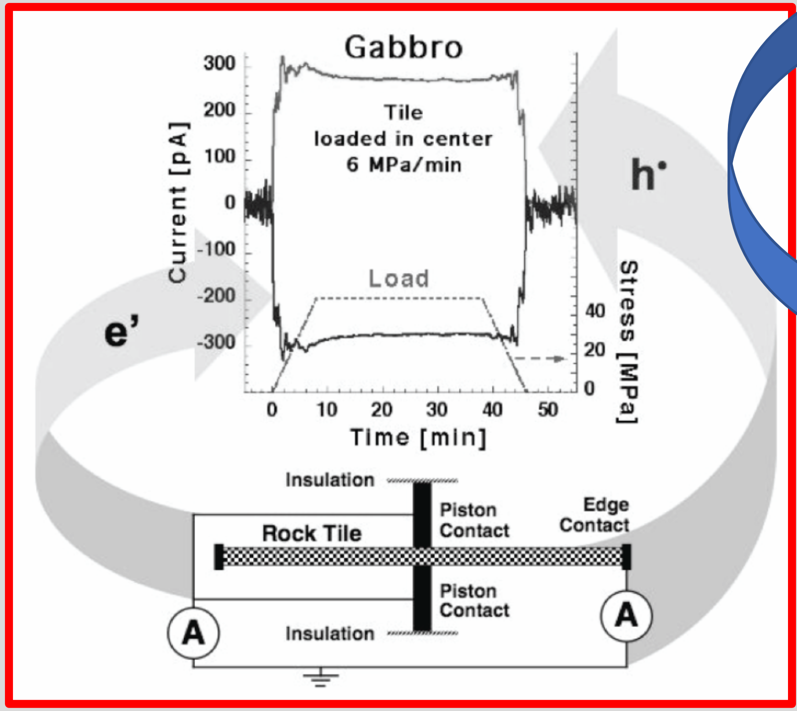

[Freund, 2007]

How to couple with?

Electrical component

Single-block COS model

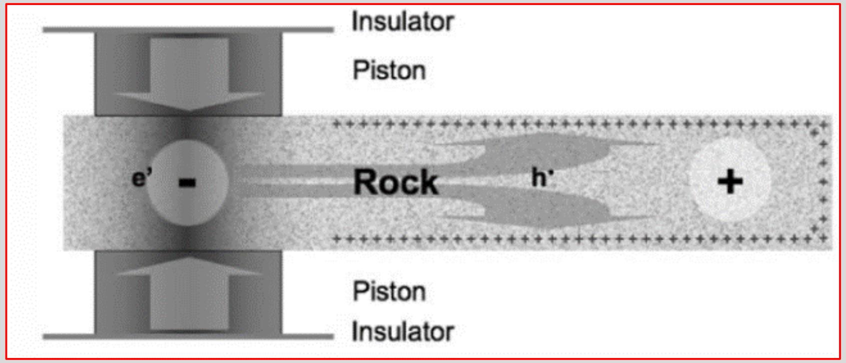

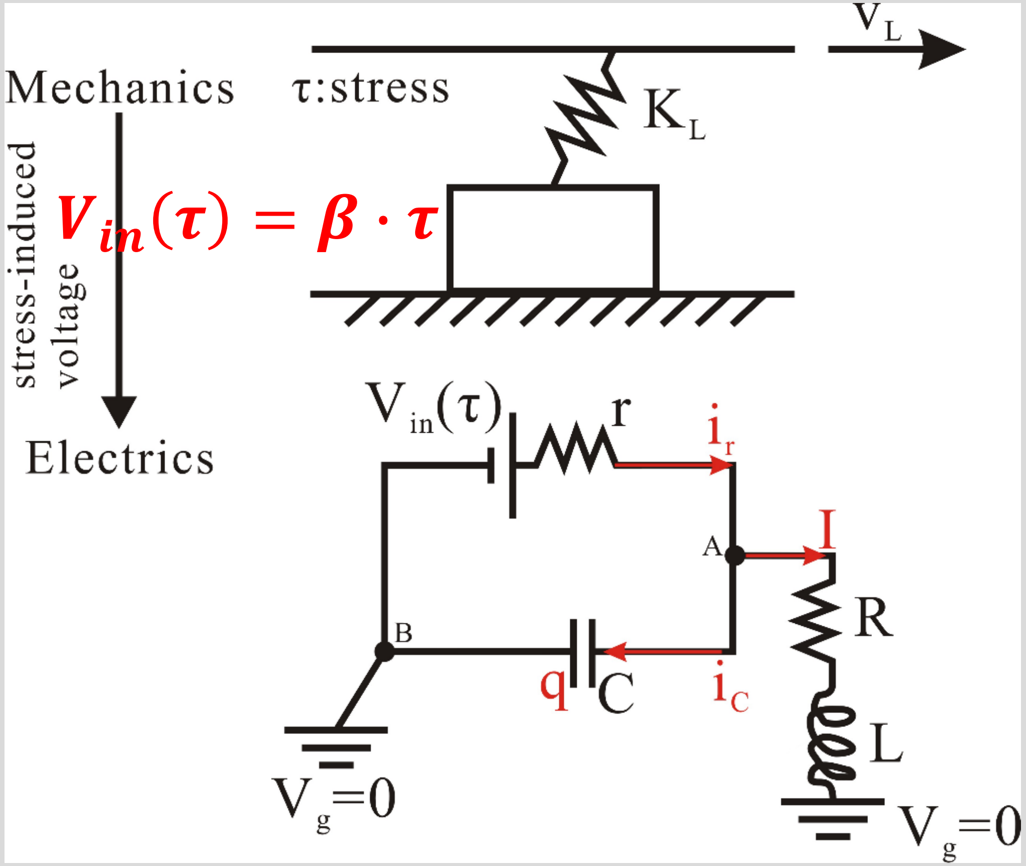

Basic principles:

(1) Kirchhoff's voltage law

$$\widehat{V_{in}} - \hat{r} i_r - \frac{q}{\hat{c}} = 0,$$

(2) Current-charge relation

$$i_c = \frac{dq}{dt},$$

(3) Kirchhoff's current law

$$i_r = I + i_c,$$

(4) Equality for the grounded part

$$I + \hat{L}\frac{dI}{dt} = \frac{q}{\hat{c}}.$$

Ranges of the Mechanical-Electrical Coefficient:

$$V_{in}(\tau) = \beta \cdot \tau$$

β is the ratio of voltage to stress, depending on materials and physical conditions, such as saturation, porosity, and temperature.

In this study, β=1.

參考文獻	岩樣	應力(MPa)	電壓(mV)	β 值
Takeuchi et al. (2006) [122]	花崗岩	50	40	0.8
Takeuchi et al. (2006) [122]	輝長岩	50	35	0.7
Takeuchi et al. (2006) [122]	斜長岩	50	80	1.6
Freund (2007) [62]	輝長岩	50	440	8.8
Freund et al. (2004) [126]	斜長岩	81	50	0.62
Hadjicontis & Mavromatou (1994) [20]	石灰石	0.5	60	120
Hadjicontis & Mavromatou (1994) [20]	石英	0.5	200	400
Hadjicontis & Mavromatou (1994) [20]	花崗岩	20	250	12.5
Yoshida et al. (1998) [127]	乾砂岩	140	950	6.79
Yoshida et al. (1998) [127]	飽和砂岩	120	180	1.5
Yoshida et al. (1998) [127]	乾玄武岩	415	10	0.02
Yoshida et al. (1998) [127]	飽和玄武岩	355	210	0.59

Analytic Solution

$$\Delta(r_c, c_c, L_c) = 0$$

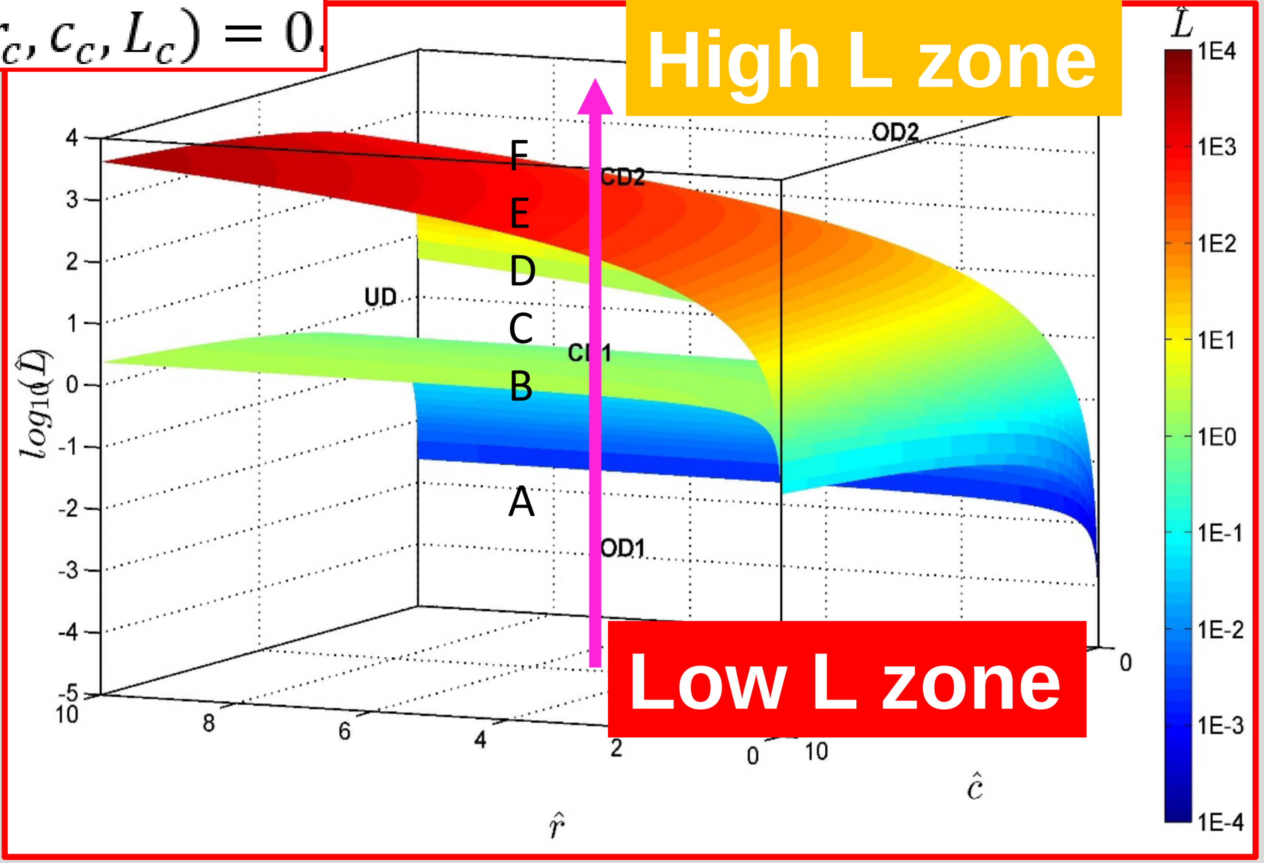

Laplace transform

$$1 - \hat{r}\tilde{i}_r - \frac{\tilde{q}}{\hat{c}} = 0,$$

$$\tilde{i}_c = s\tilde{q},$$

$$\tilde{i}_r = \tilde{I} + \tilde{i}_c,$$

$$\tilde{I} + \hat{L}s\tilde{I} = \frac{\tilde{q}}{\hat{c}},$$

$$\tilde{q}(s) = \frac{\left(s+\frac{1}{\hat{L}}\right)}{\hat{r}\left[s^2+\left(\frac{1}{\hat{r}\hat{c}}+\frac{1}{\hat{L}}\right)s+\left(\frac{1}{\hat{r}\hat{c}\hat{L}}+\frac{1}{\hat{c}\hat{L}}\right)\right]}.$$

$$\zeta = \frac{1}{\hat{r}\hat{c}} + \frac{1}{\hat{L}}, \quad \eta = \frac{1}{\hat{r}\hat{c}\hat{L}} + \frac{1}{\hat{c}\hat{L}}, \quad \text{and} \quad \Delta = \zeta^2 - 4\eta$$

Case 1 (Δ>0) - overdamping solution:

$$q_{gf}^{(od)}(t) = \frac{e^{\frac{-\zeta+\sqrt{\Delta}}{2}t}\left(\frac{-\zeta+\sqrt{\Delta}}{2}+\frac{1}{\hat{L}}\right)+e^{\frac{-\zeta-\sqrt{\Delta}}{2}t}\left(-\frac{1}{\hat{L}}-\frac{-\zeta-\sqrt{\Delta}}{2}\right)}{\hat{r}\sqrt{\Delta}}.$$

Case 2 (Δ=0) - critical damping solution:

$$q_{gf}^{(cd)}(t) = \frac{e^{-\frac{\zeta}{2}t}\left[t\left(-\frac{\zeta}{2}+\frac{1}{\hat{L}}\right)+1\right]}{\hat{r}}.$$

Case 3 (Δ<0) - underdamping solution:

$$q_{gf}^{(ud)}(t) = \frac{e^{-\frac{\zeta}{2}t}\left[\omega\cos(\omega t)+\left(-\frac{\zeta}{2}+\frac{1}{\hat{L}}\right)\sin(\omega t)\right]}{\omega\hat{r}}, \quad \omega = \frac{\sqrt{|\Delta|}}{2}$$

The determinant forms an electric phase space.

	Set	$\hat{r}$	$\hat{c}$	$\hat{L}$	Damping Region	ζ	η	Δ	ω
Low L	A	5	5	0.1	OD1	10.04	2.40	91.20	
	B	5	5	1.14	CD1	0.92	0.21	0	
	C	5	5	10	UD	0.14	0.024	-0.0764	0.14
High L	D	5	5	100	UD	0.05	0.0024	-0.0071	0.04
	E	5	5	548.86	CD2	0.418	4.37E-4	0	
	F	5	5	700	OD2	0.414	3.43E-4	3.45E-4	

Multi-blocks COS model

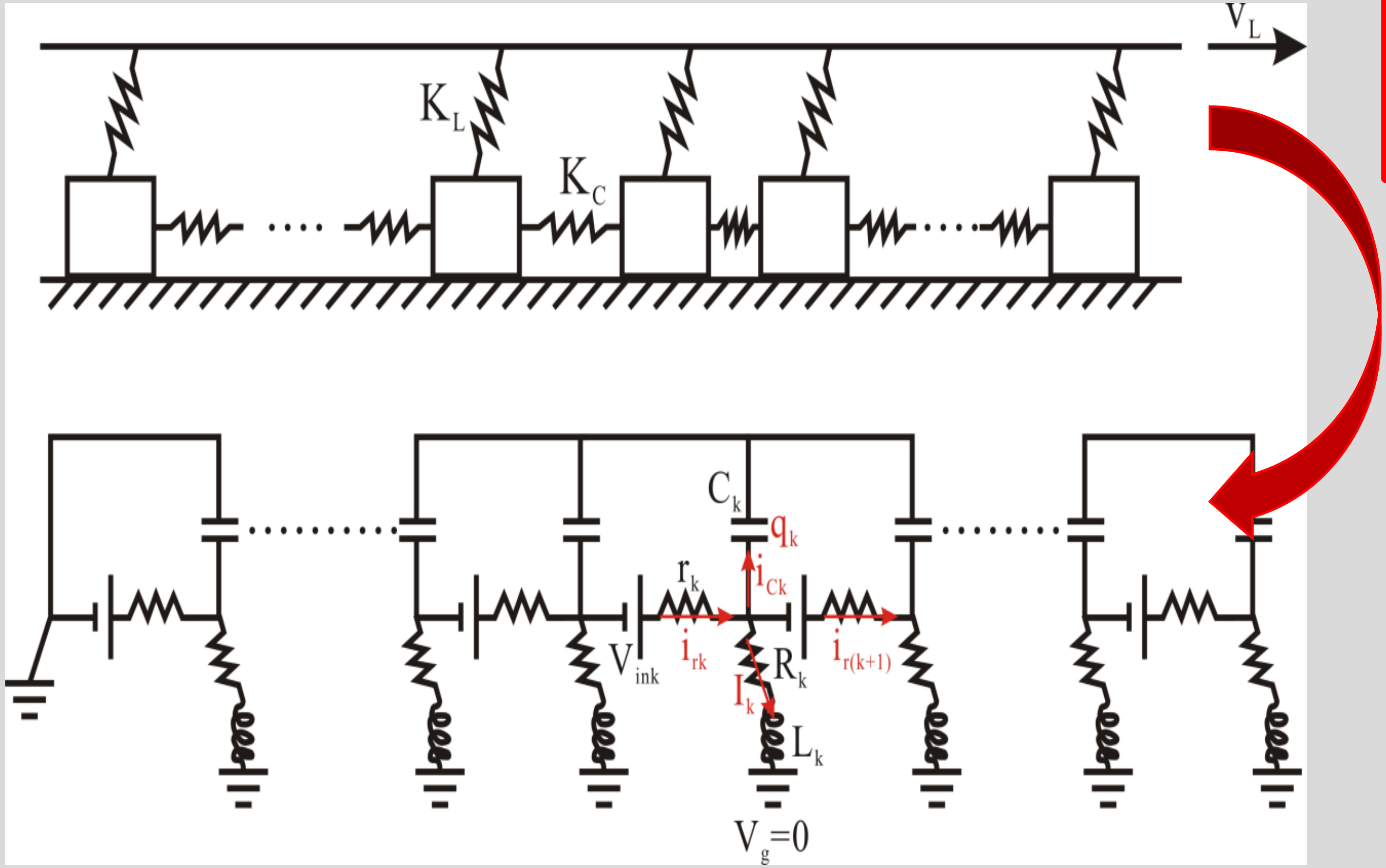

Stress-induced voltage:

$$V_{ink}(\tau_k) = p_{dk}\beta_k\tau_k,$$

$$p_{dk} = \begin{cases} 1\ , \tau_{k-1} \geq \tau_{k+1} \\ -1, \tau_{k-1} \leq \tau_{k+1} \end{cases}$$

Considering polarization

(1) Kirchhoff's voltage law

$$\begin{cases} V_{in1} - i_{r1}r_1 - \frac{q_1}{c_1} = 0 \\ V_{ink} - i_{rk}r_k - \frac{q_k}{c_k} + \frac{q_{k-1}}{c_{k-1}} = 0, \qquad k = 2 \text{ to } N \end{cases}$$

(2) Current-charge relation

$$i_{ck} = \frac{dq_k}{dt}, \qquad k = 1 \text{ to } N.$$

(3) Kirchhoff's current law

$$\begin{cases} i_{rk} = I_k + i_{ck} + i_{r(k+1)}, \qquad k = 1 \text{ to } N-1 \\ i_{rN} = I_N + i_{cN} \end{cases}$$

(4) Equality for the grounded part

$$\begin{cases} I_1R_1 + \frac{dI_1}{dt}L_1 = V_{in1} - i_{r1}r_1 \\ I_kR_k + \frac{dI_k}{dt}L_k - I_{k-1}R_{k-1} - \frac{dI_{k-1}}{dt}L_{k-1} = V_{ink} - i_{rk}r_k, \qquad k = 2 \text{ to } N \end{cases}$$

(5) Total voltage of the system

$$V_{SB} = \frac{1}{N}\sum_{k=1}^{N}\left(R_kI_k + L_k\frac{dI_k}{dt}\right) = \frac{1}{N}\sum_{k=1}^{N}\frac{q_k}{c_k}.$$

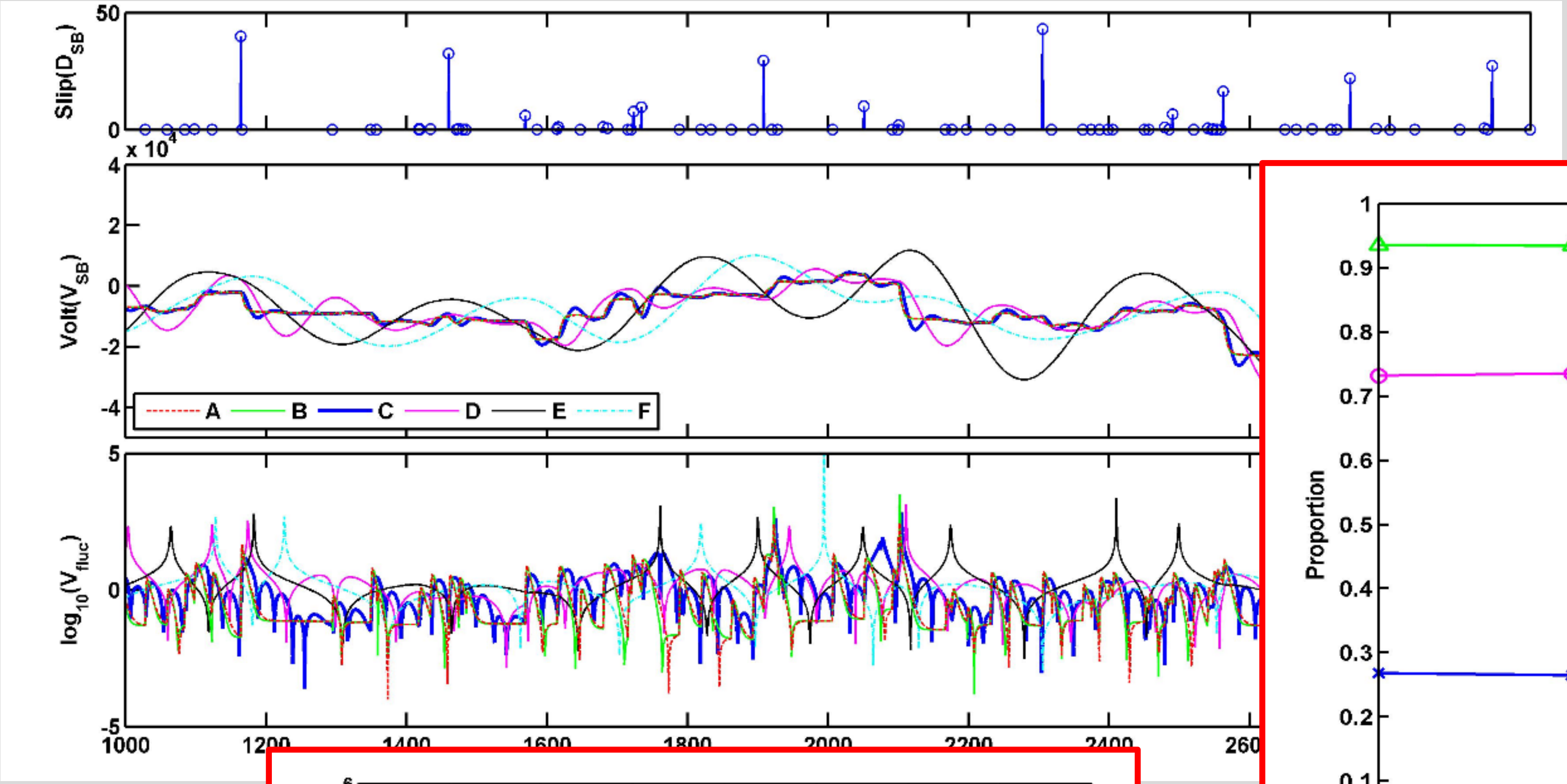

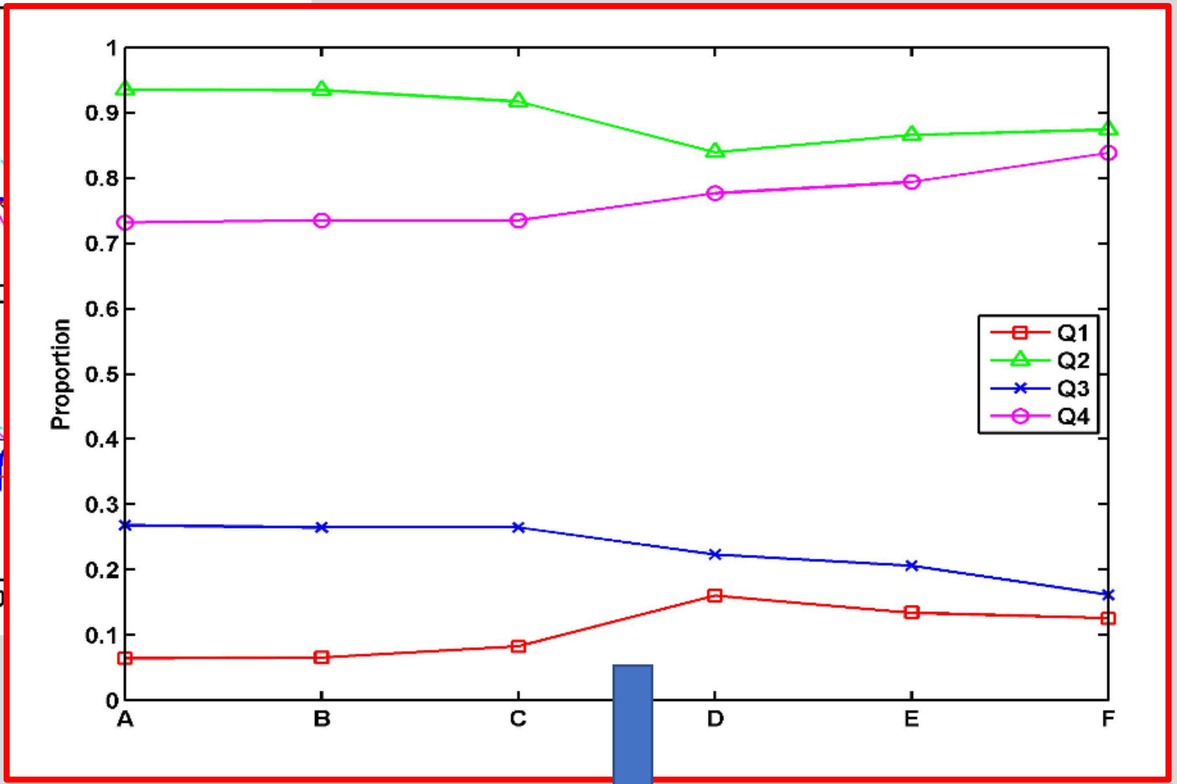

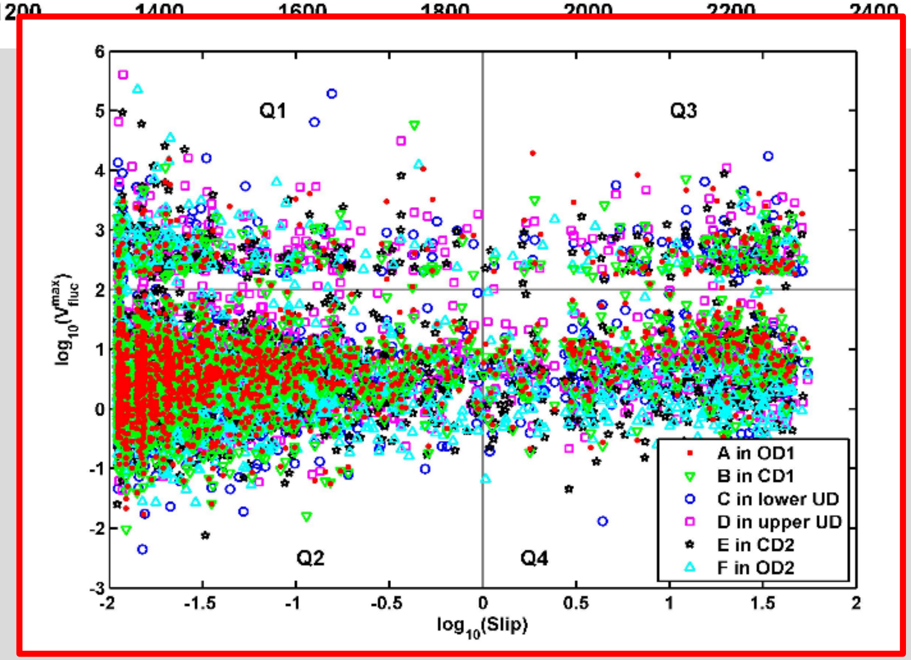

1) Q2>Q1: small events generate most of small voltage fluctuations.
2) Q4>Q3: large events do not usually generate large voltage variance.
3) Transition: between the upper and lower UD.

Skewness & Kurtosis Anomalies

Simulations

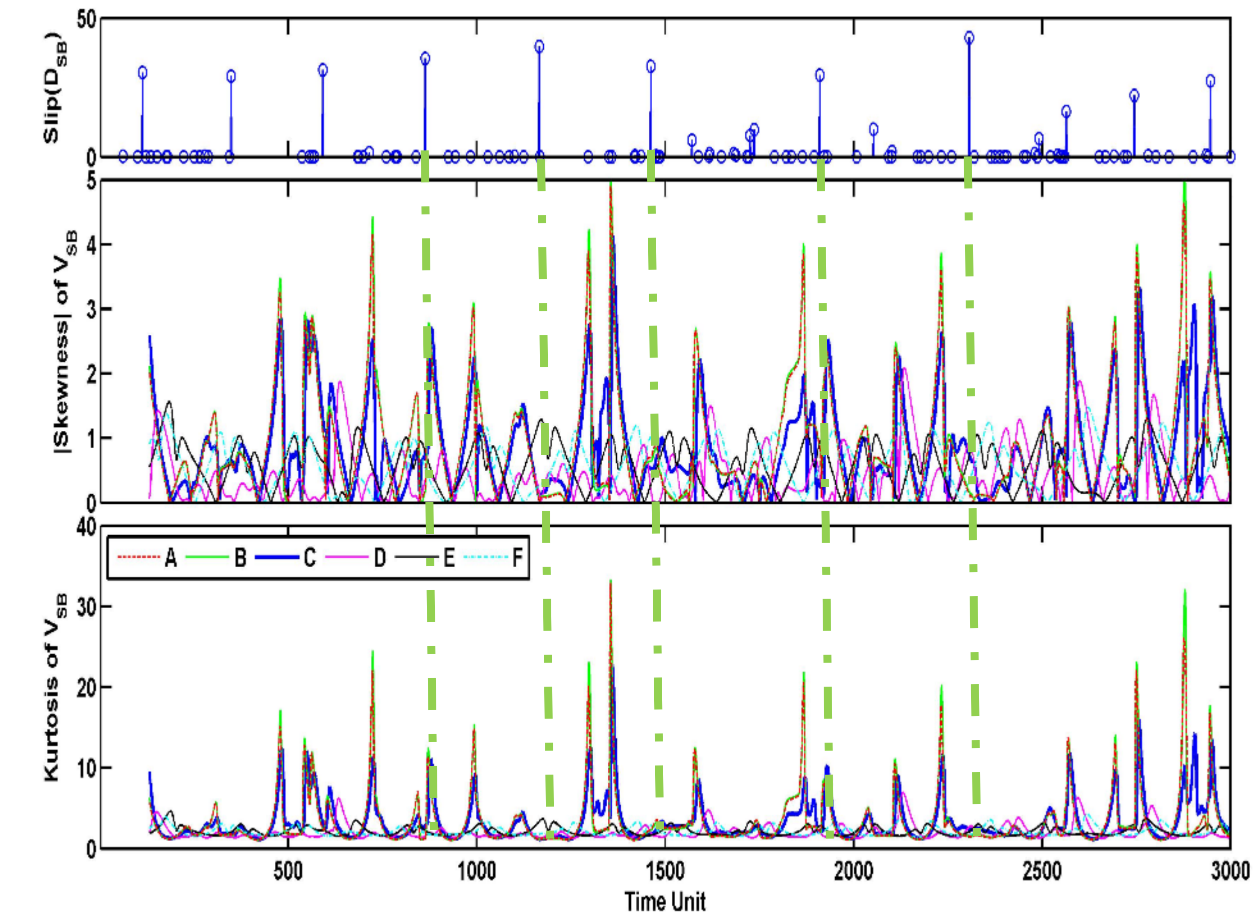

Observations

2012-2013 PULI station

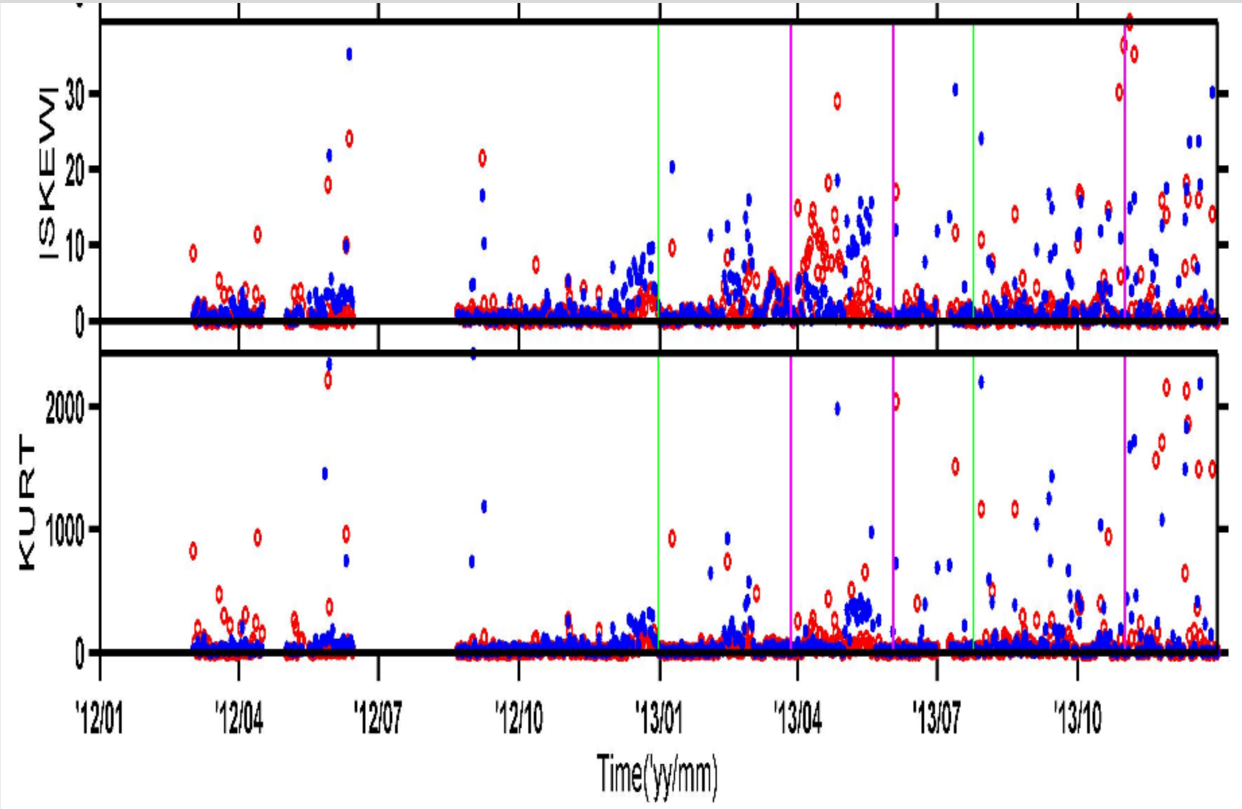

Electric signals:

1) be skewed by fracture-induced signals
2) be concentrated by fracture-induced signals

Power Spectral Analysis

Simulations

$$P(f) = af^{-b}$$

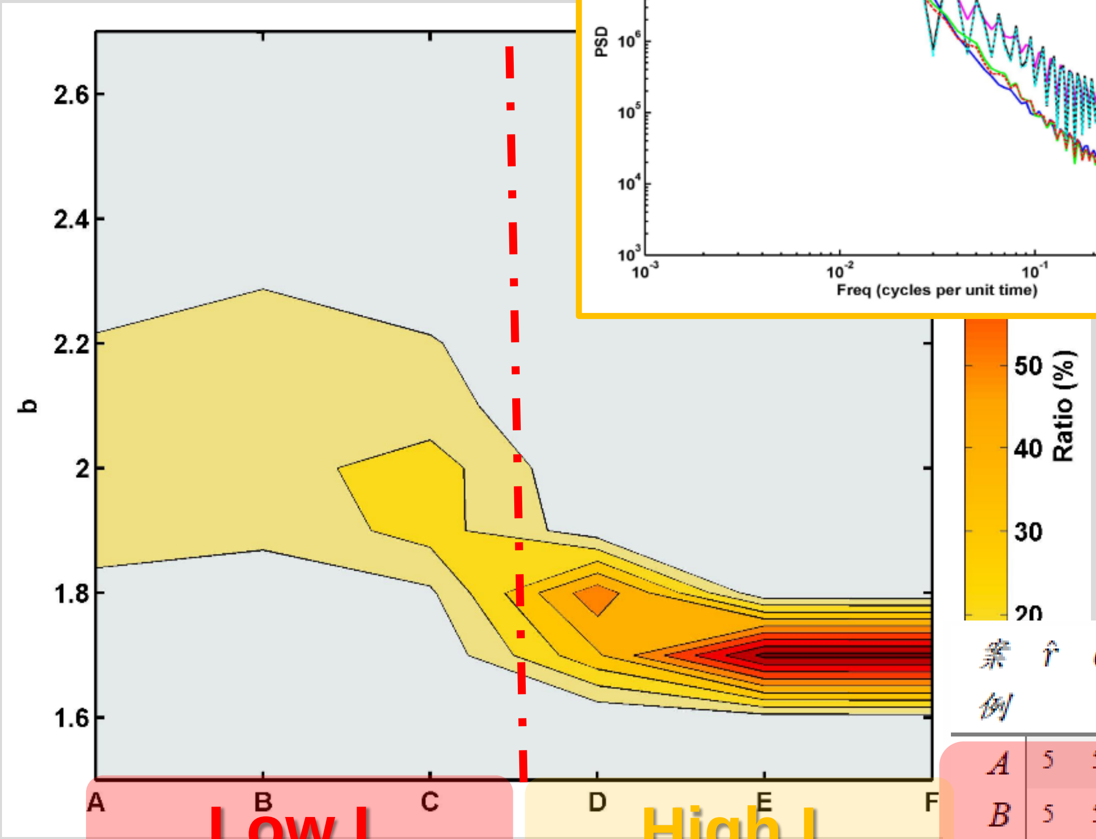

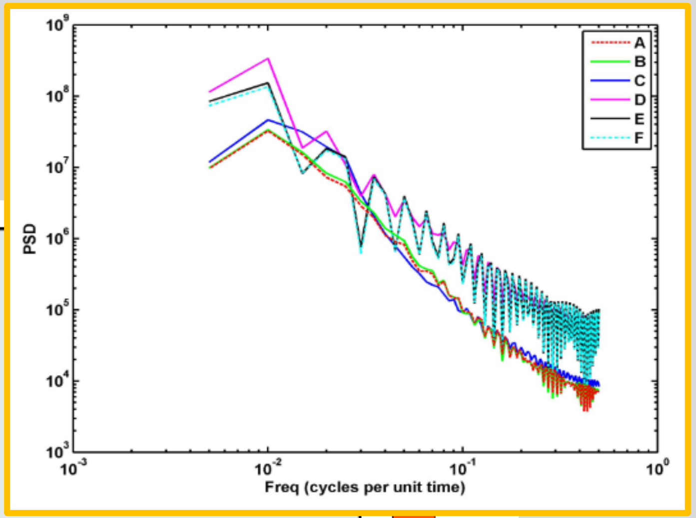

Low L

High L

案例	$\hat{r}$	$\hat{c}$	$\hat{L}$	阻尼區	Δ	b (斜率)
A	5	5	0.1	OD1	91.20	2.12±0.39
B	5	5	$\hat{L}_{c1}$	CD1	0	2.16±0.42
C	5	5	10	UD	-0.0764	2.05±0.24
D	5	5	100	UD	-0.0071	1.77±0.04
E	5	5	$\hat{L}_{c2}$	CD2	0	1.72±0.03
F	5	5	700	OD2	[illegible].45E-4	1.72±0.03

Low L

High L

Observations

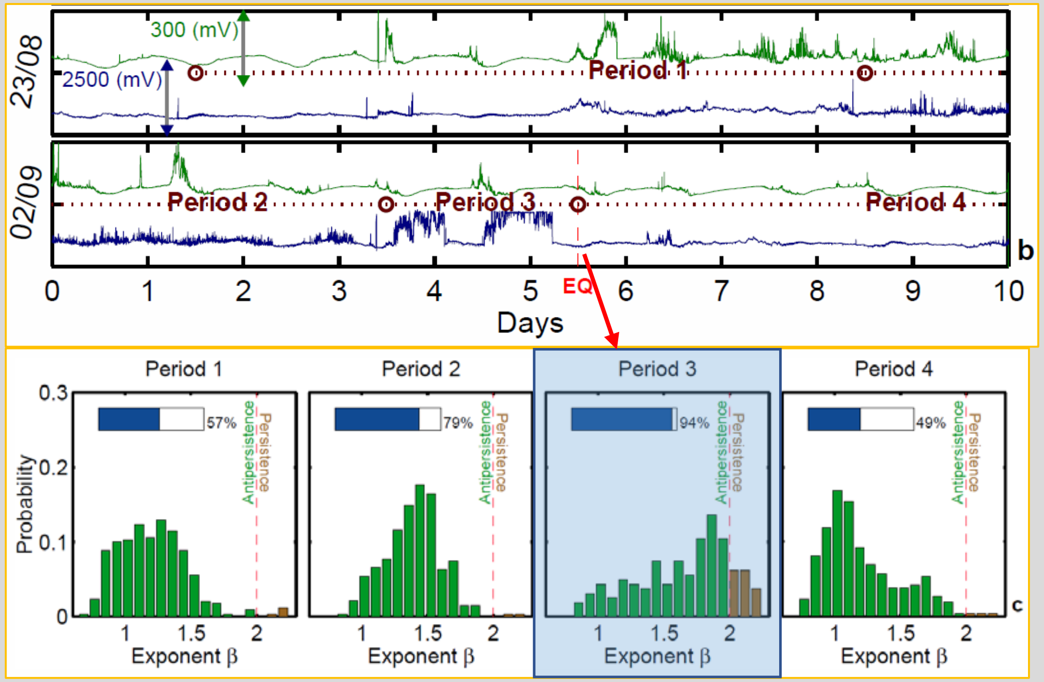

[Eftaxias et al., 2003]

1) Transition: between the upper and lower UD

2) Local stress states change earth electrokinetic states in different earthquake preparation phases

Summary of COS Model Analysis

- **Seismoelectric model:** spring-block system (mechanical component) + RLC circuit system (electrokinetic component), provides general theoretical framework for modeling and analyzing geoelectric precursors to earthquakes.

- Explanation:
  1) Skewness and kurtosis anomalies
  2) PSD's power-law exponent transitions prior to large earthquakes.

- Precursory electromagnetic signals may be observed before large events if
  1) there are small foreshocks, i.e. small earthquakes that would be too small to be detected seismically;
  2) the local electrokinetic damping conditions allow them to leave a measurable electromagnetic fingerprint.

Observation (I): Long-term Behavior for Correlations between Mechanics and Electrics in the Crust

Purpose:

Analyzing self-potential signals related to natural and anthropogenic factors

Data:

- **Self-potential:**
  - 20 stations evenly distributed in Taiwan
  - sampling rate: 15 points per second
  - from 2012 to 2017
- **Earthquake:**
  - all events
  - from 2012 to 2017
- **GPS:**
  - from 2012 to 2017
  - downloaded from the GPSLAB
  - processed with GIPSY-OASIS software
- **Urbanization:**
  - values from 1 to 5
  - estimated by Huang et al., 2018

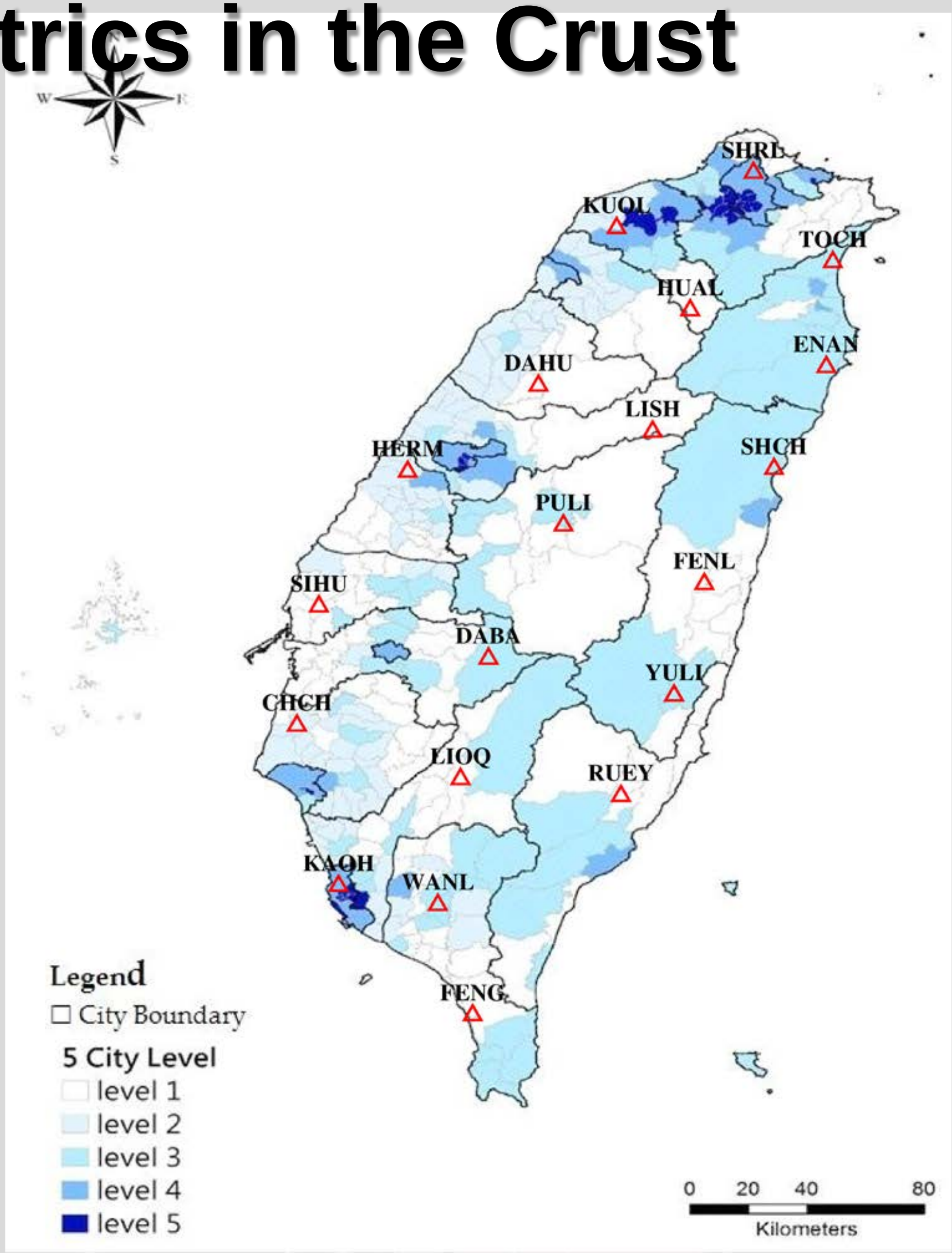

Processing of Self-Potential Data

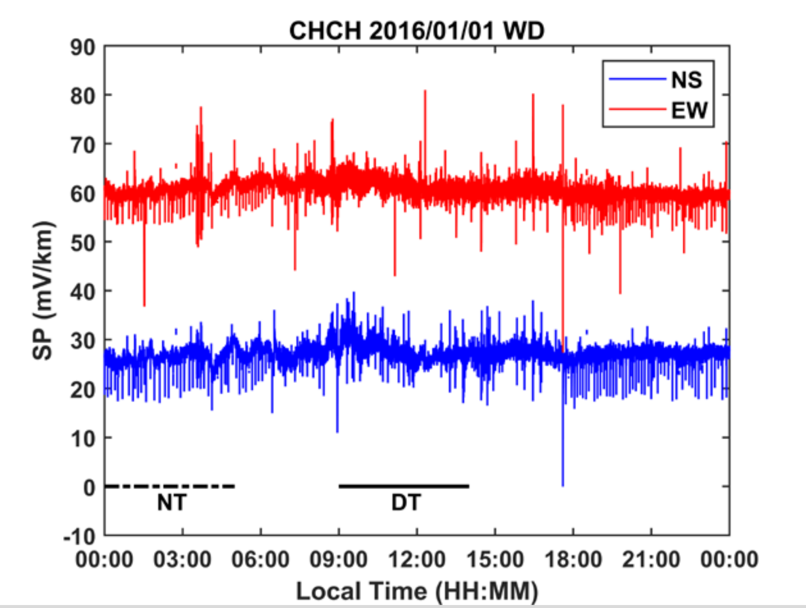

$$P(f) = \alpha f^{-\beta}$$

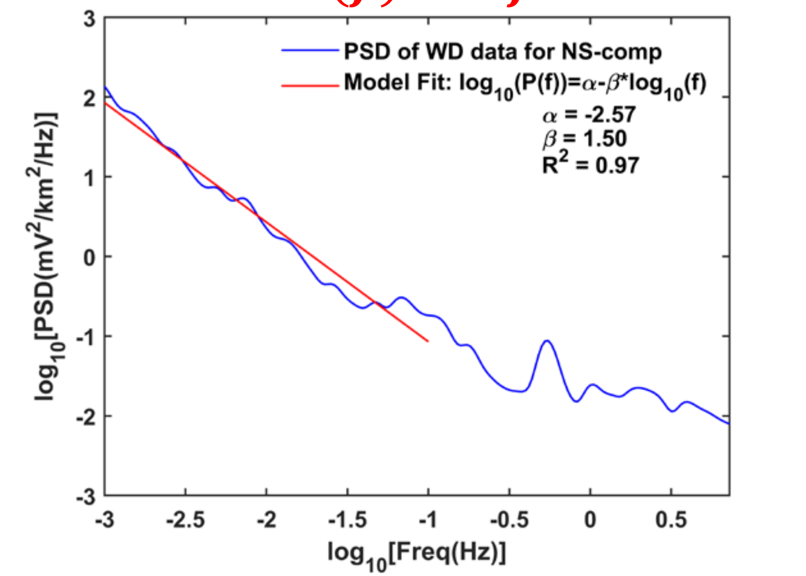

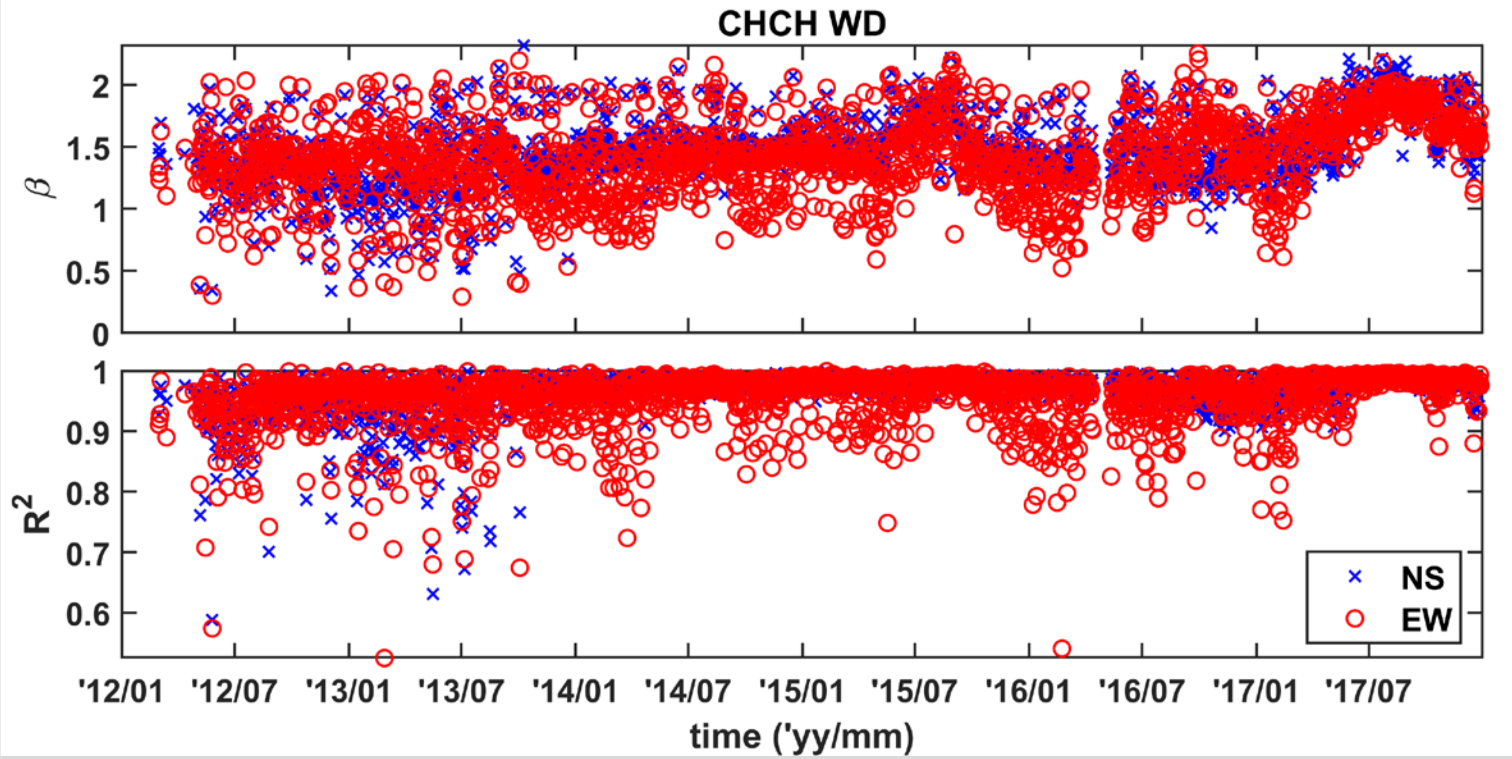

Take the average for β with R^2>0.8:

$\beta_{WD,NS}$ = 1.48±0.26

$\beta_{WD,EW}$ = 1.42±0.31

The average β with different frequency bands will be calculated.

Spatial Distributions of SP Exponent, b-value, and Dilation Rate

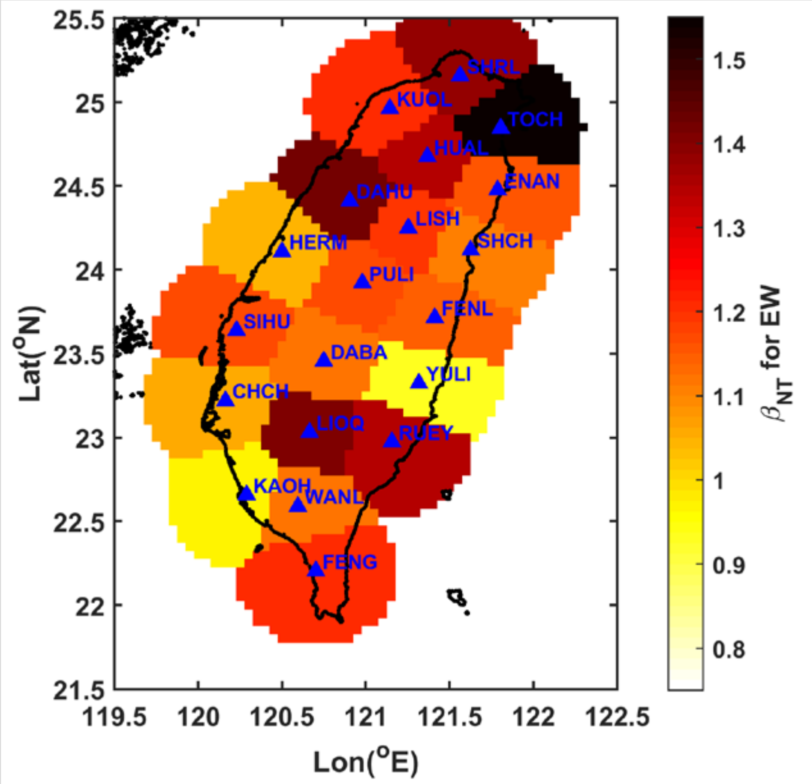

Self-potential power-law exponent
$\beta_{NT,EW}$ with f = 0.001- 0.1 Hz

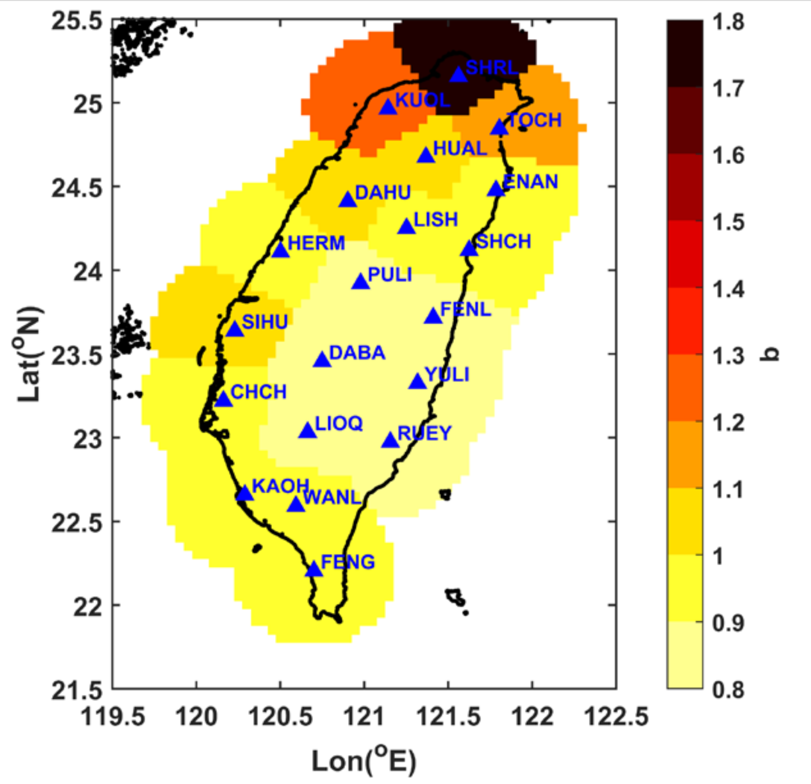

Gutenberg-Richter b-value
Epicentral distance to stations:
R_{thr} = 50 km

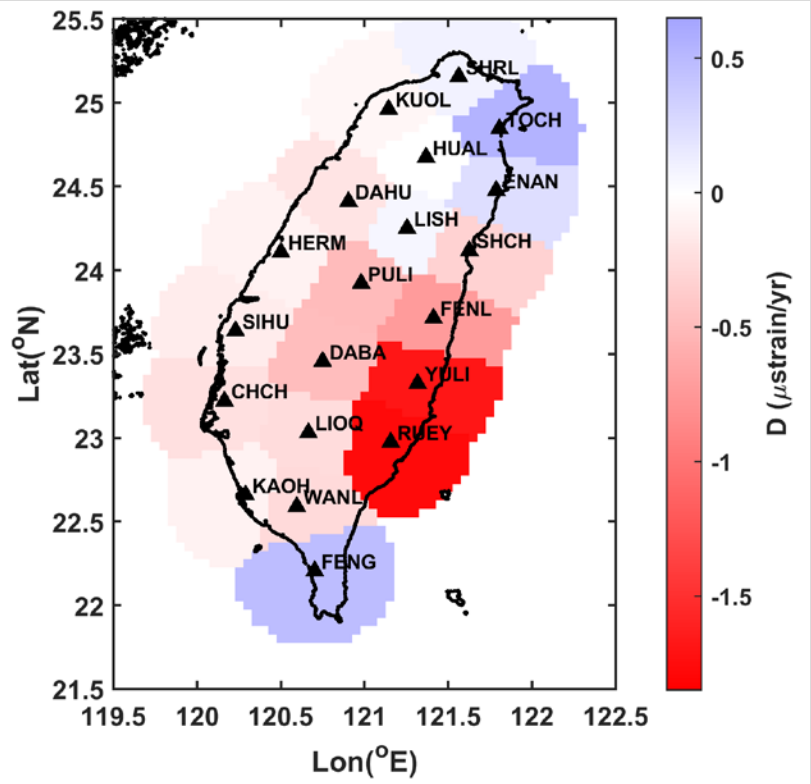

Dilation strain rate

Self-potential power-law parameters with f = 0.001- 0.1 Hz

Correlation Matrix EW

	α_{WD}	β_{WD}	α_{DT}	β_{DT}	α_{NT}	β_{NT}	U	b	D
α_{WD}	1.00	-0.35	0.92	-0.39	0.89	-0.19	-0.04	0.07	0.08
β_{WD}	-0.35	1.00	-0.22	0.81	-0.12	0.88	-0.63	0.09	-0.03
α_{DT}	0.92	-0.22	1.00	-0.44	0.81	-0.08	-0.04	0.08	0.07
β_{DT}	-0.39	0.81	-0.44	1.00	-0.20	0.74	-0.57	-0.03	-0.03
α_{NT}	0.89	-0.12	0.81	-0.20	1.00	-0.09	-0.30	-0.02	0.02
β_{NT}	-0.19	0.88	-0.08	0.74	-0.09	1.00	-0.48	0.30	0.03
U	-0.04	-0.63	-0.04	-0.57	-0.30	-0.48	1.00	0.39	0.10
b	0.07	0.09	0.08	-0.03	-0.02	0.30	0.39	1.00	0.41
D	0.08	-0.03	0.07	-0.03	0.02	0.03	0.10	0.41	1.00

Correlation Matrix NS

	α_{WD}	β_{WD}	α_{DT}	β_{DT}	α_{NT}	β_{NT}	U	b	D
α_{WD}	1.00	-0.27	0.94	-0.38	0.88	-0.17	-0.15	-0.10	-0.10
β_{WD}	-0.27	1.00	-0.18	0.89	-0.05	0.89	-0.65	-0.06	0.15
α_{DT}	0.94	-0.18	1.00	-0.36	0.79	-0.07	-0.17	-0.13	-0.16
β_{DT}	-0.38	0.89	-0.36	1.00	-0.20	0.85	-0.47	0.09	0.33
α_{NT}	0.88	-0.05	0.79	-0.20	1.00	-0.11	-0.38	-0.18	-0.13
β_{NT}	-0.17	0.89	-0.07	0.85	-0.11	1.00	-0.57	0.10	0.27
U	-0.15	-0.65	-0.17	-0.47	-0.38	-0.57	1.00	0.39	0.10
b	-0.10	-0.06	-0.13	0.09	-0.18	0.10	0.39	1.00	0.41
D	-0.10	0.15	-0.16	0.33	-0.13	0.27	0.10	0.41	1.00

Frequency dependence

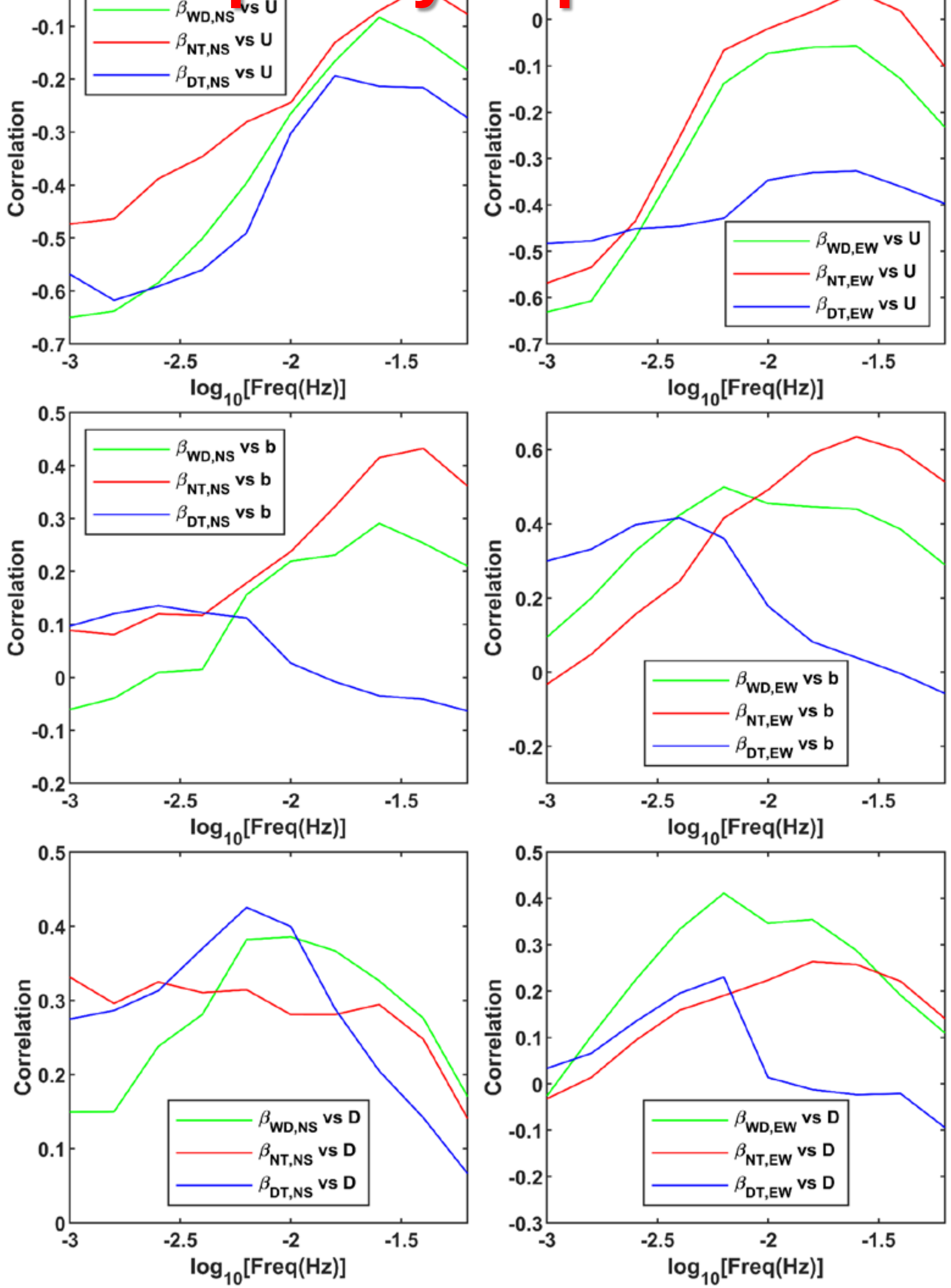

Summary of Long-term Seismo-Electromagnetic Behavior

- The moderate correlation exists between b-value and dilation rate, in agreement with a fact that crustal deformation affects the fractal behavior in the crust (Öncel & Wilson, 2004).
- The self-potential signals with ***f* = 0.006-1 Hz** are correlated with mechanics in the crust, but less correlated with human-made noises.
- The determination of the optimal frequency band allows us to filter and screen the self-potential signals and improve the quality of the analyses.

Observation (II): Pre-earthquake Anomalies of Geoelectric Monitoring System (GEMS)

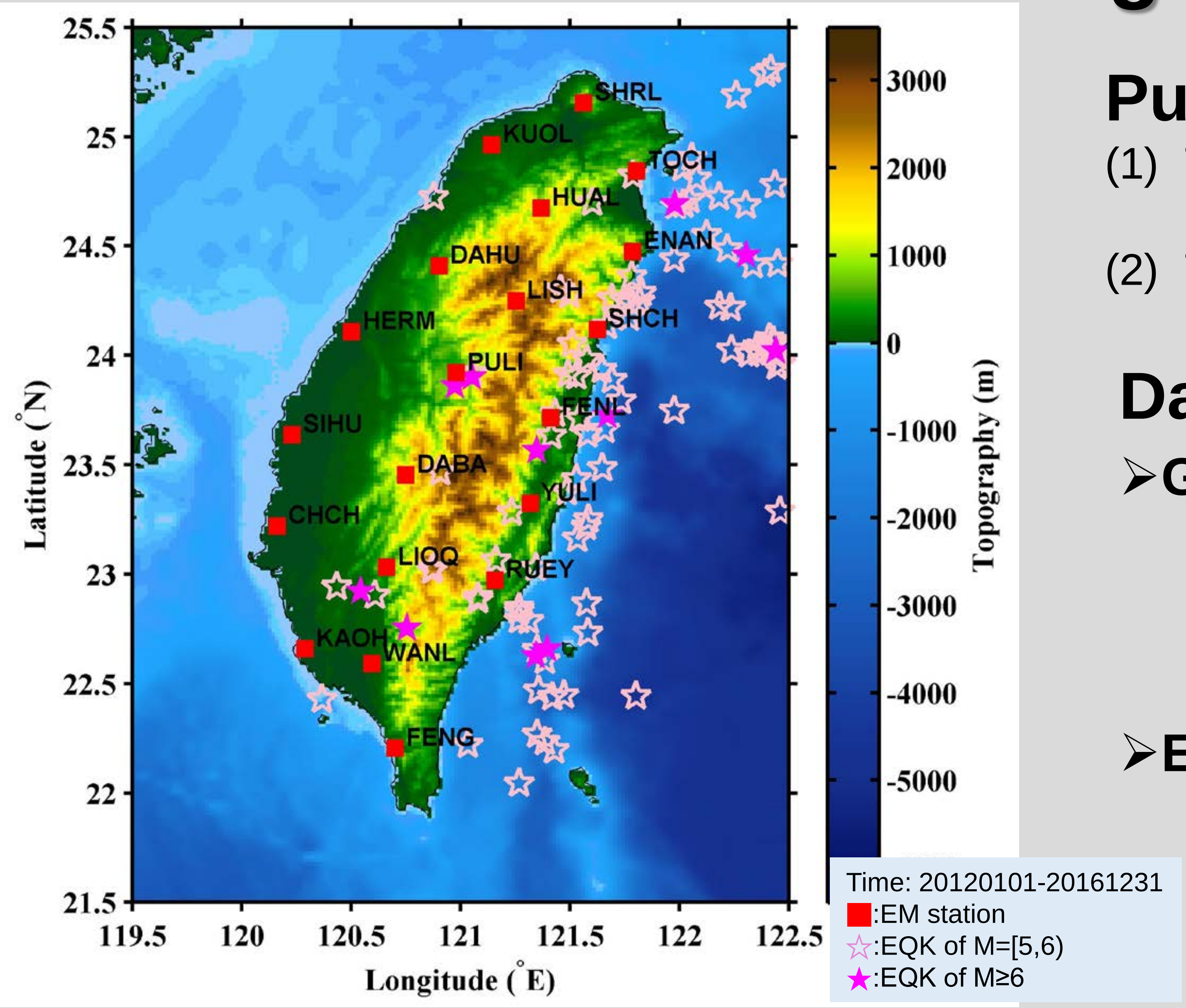

Purpose:

(1) To test relationships between geoelectrics and earthquakes

(2) To build up short-term earthquake forecasts

Data:

➢GEMS:

- 20 stations evenly distributed in Taiwan
- Continuous, real time data
- from 2012 to 2016

➢Earthquake:

- 105 $M_L \geq 5$ EQKs
- from 2012 to 2016

Data Analysis of Geoelectric Time Series

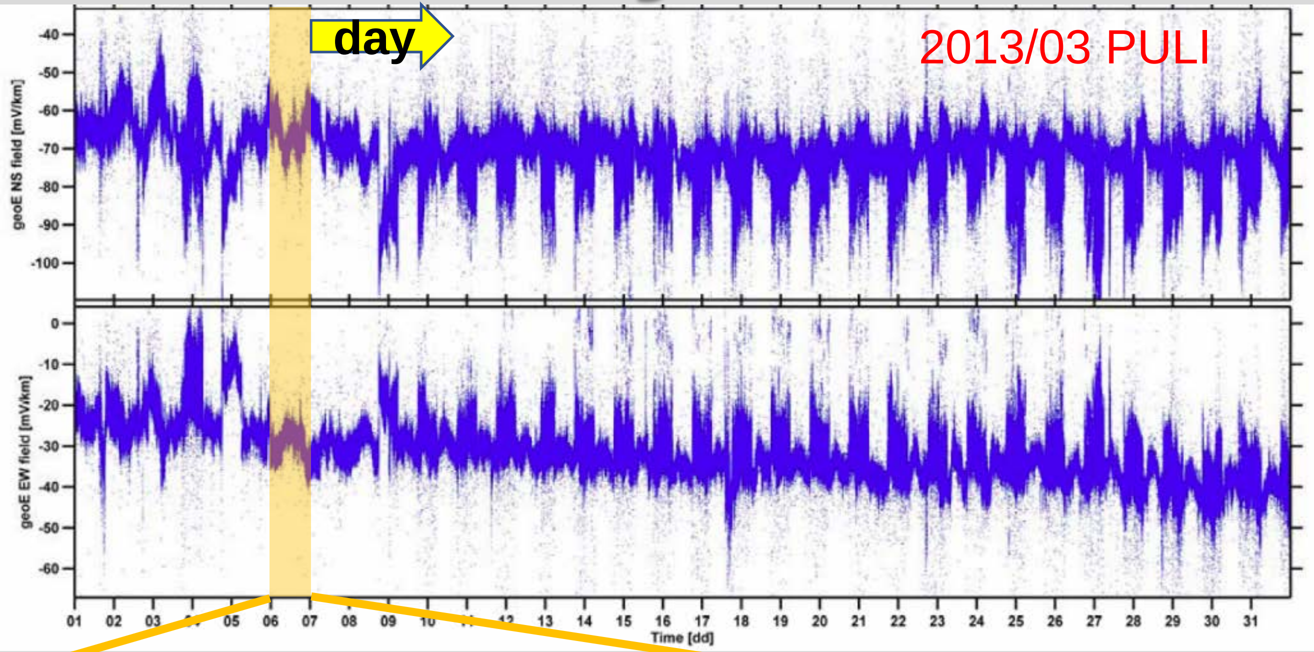

Selected Statistics

- Mean
- Variance (V): Broadness
- Skewness (S): Symmetry
- Kurtosis (K): Tailedness

$$V = \frac{\sum_{i=1}^{n}(x_i - \mu)^2}{n-1}$$

$$S = \frac{\frac{1}{n}\sum_{i=1}^{n}(x_i - \mu)^3}{\left(\sqrt{\frac{1}{n}\sum_{i=1}^{n}(x_i - \mu)^2}\right)^3}$$

$$K = \frac{\frac{1}{n}\sum_{i=1}^{n}(x_i - \mu)^4}{\left(\frac{1}{n}\sum_{i=1}^{n}(x_i - \mu)^2\right)^2}$$

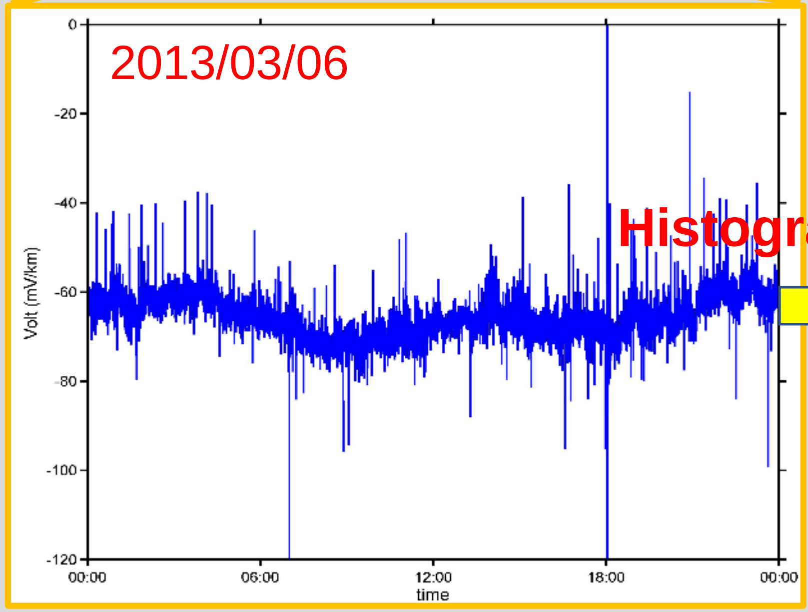

Histogram of the series

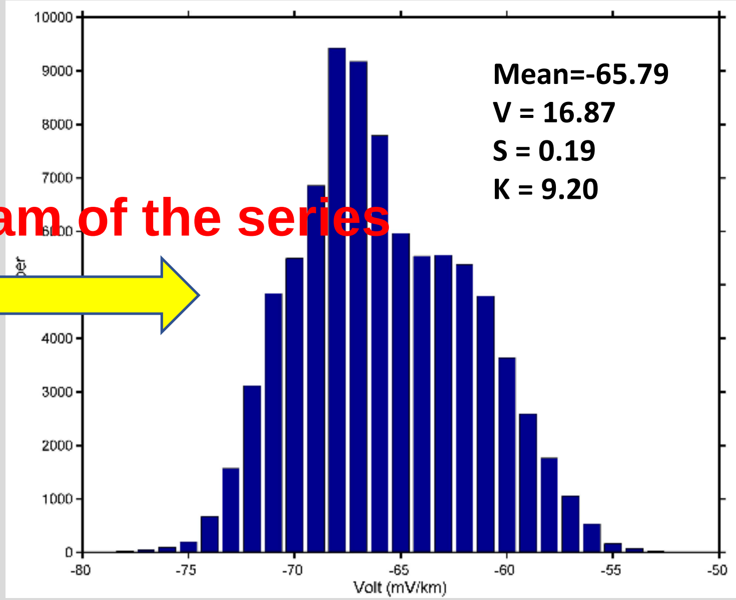

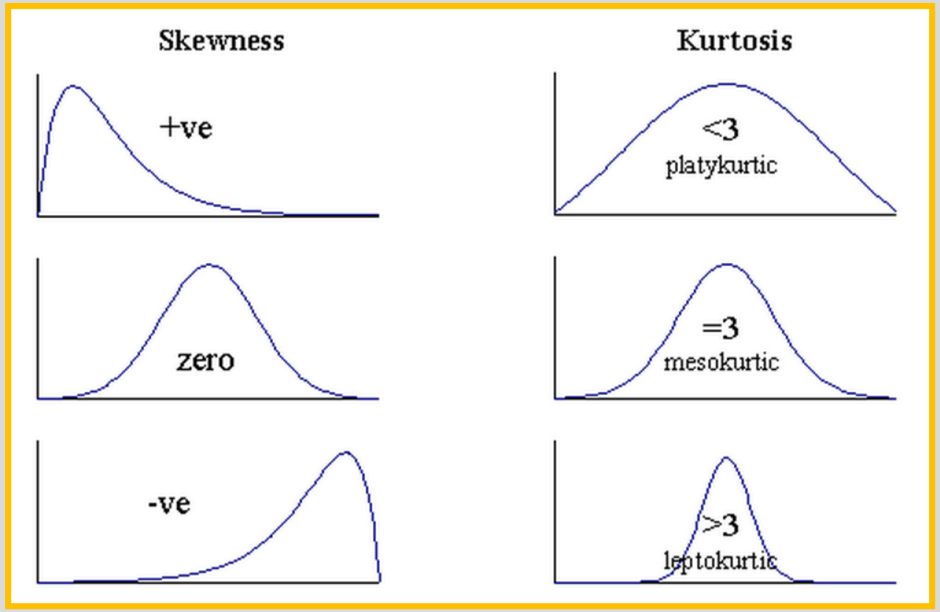

Statistical time series for 2013 Puli M6 EQs

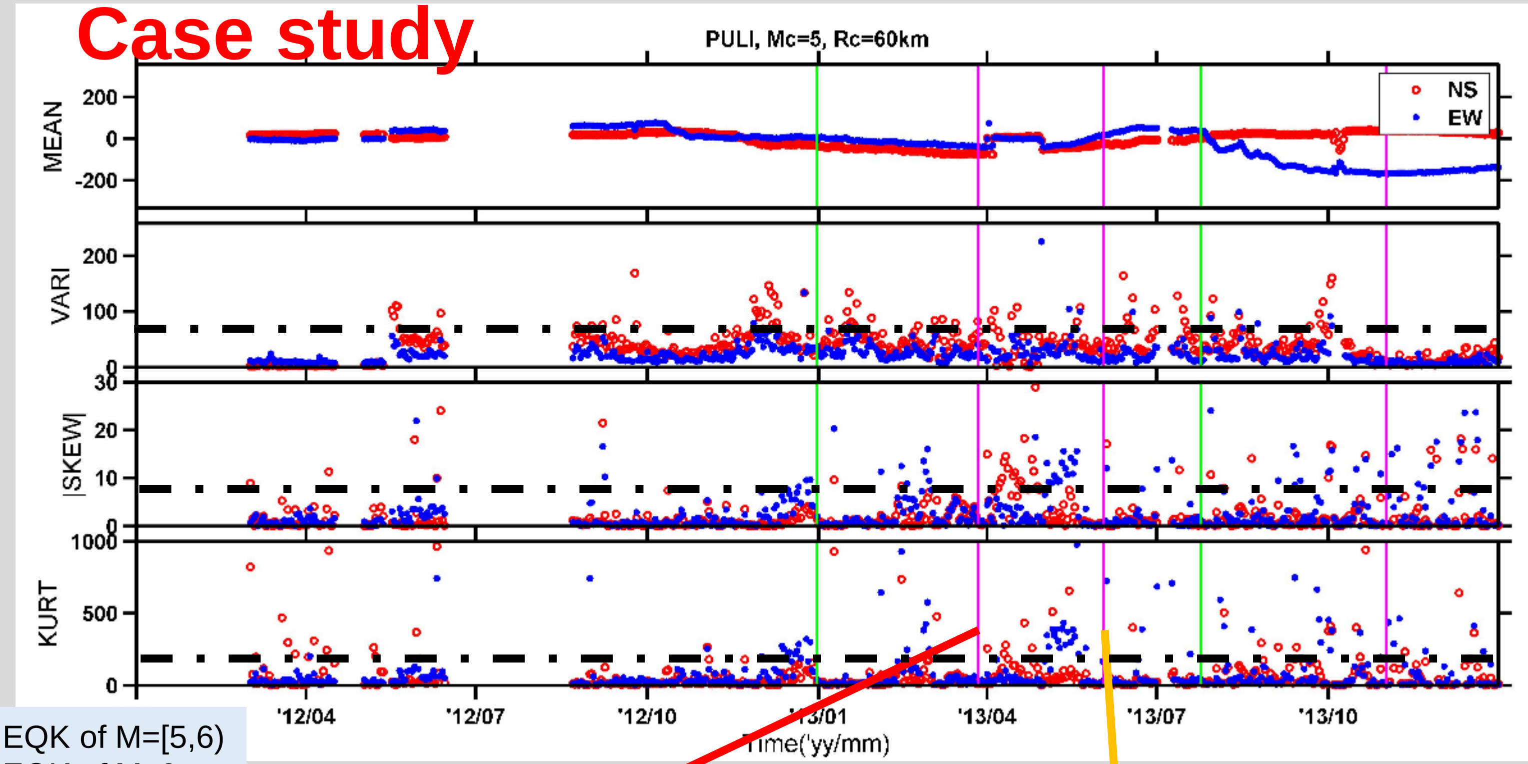

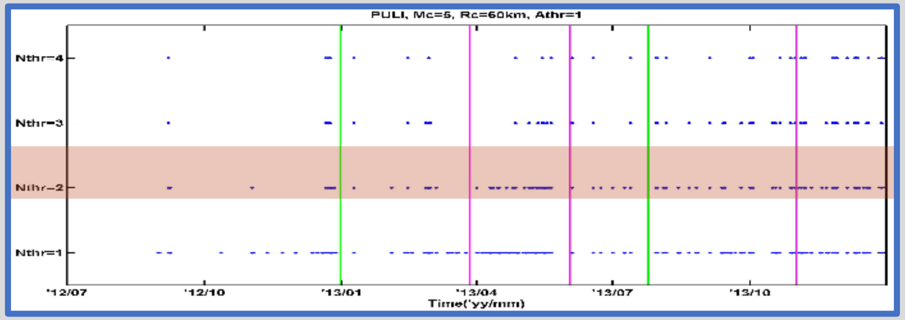

:EQK of M=[5,6)

:EQK of M≥6

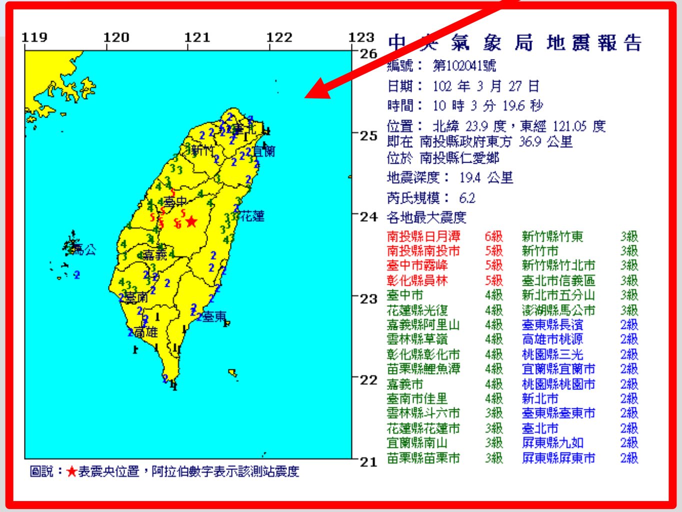

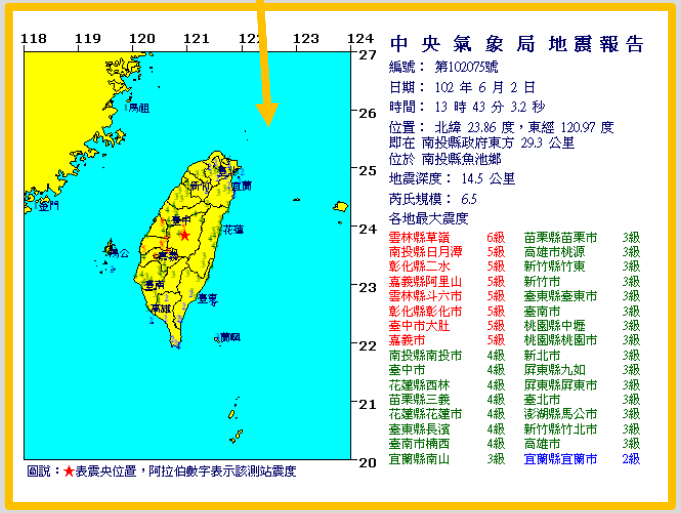

For 2013/3/27 M6 EQ,
[1] Distance: ***~21km***
[2] Lead Time: ***21days***
[3] Anomaly Ratio: ***7days/30days***

For 2013/6/2 M6 EQ,
[1] Distance: ***~16km***
[2] Lead Time: ***12days***
[3] Anomaly Ratio: ***19days/30days***

1. Skewness and kurtosis appear anomalous before the two M6 earthquakes.

2. The crustal system undergo critical states in the earthquake preparation process.

Geoelectric Monitoring System's Time of Increased Probability (GEMSTIP): Two-phase optimization

Drawback in previous studies:

- **Case Study:**
  No significance
- **Superposed Epoch Analysis:**
  Ignoring false alarms
- **One-Phase Optimization:**
  No testing study;
  Retrospective studies
  only in "training phases"

In this study

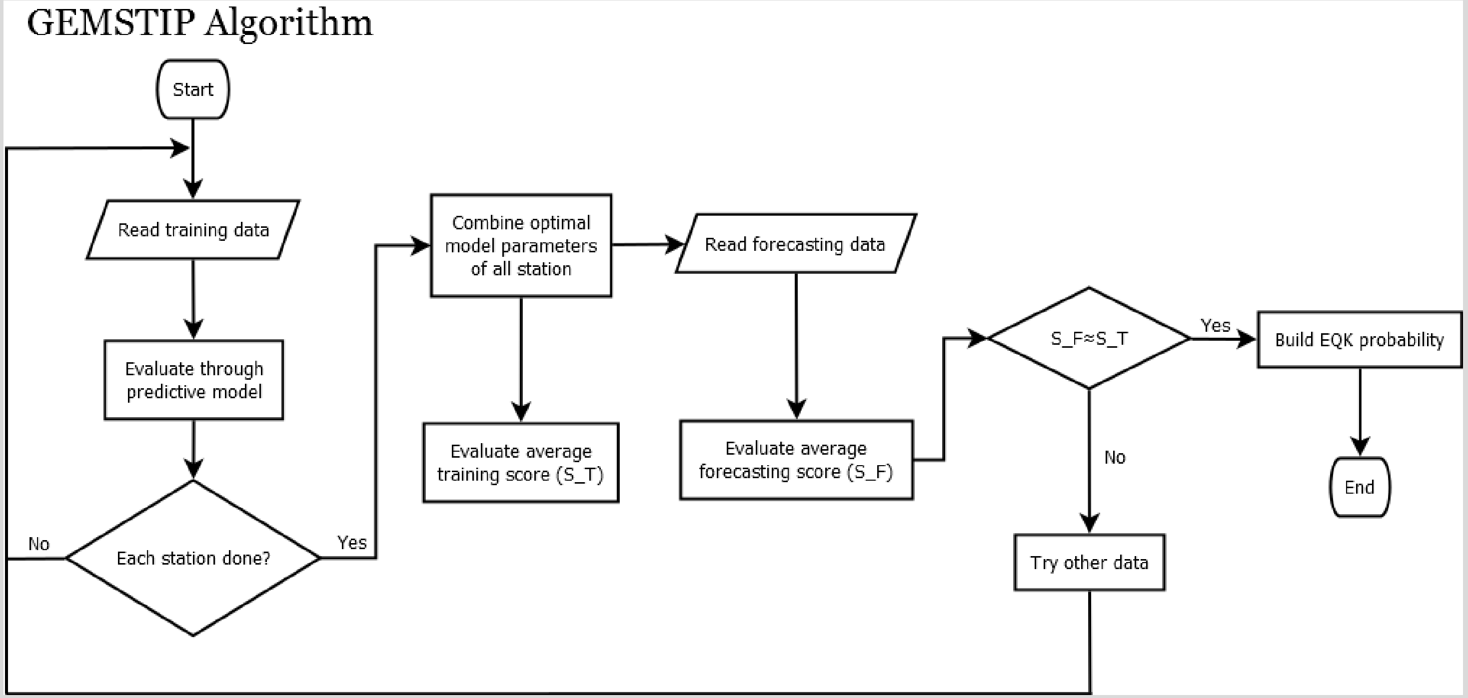

(1) After the training phase, **true forecasts** can be proposed, which consist in selecting the optimal model parameters and applying them to an independent dataset.
(2) Any prediction/forecasting method should be qualified by its reliability and skill within at least two independent phases: a training phase and a testing phase.

Step 1: Data & Targets

Data: Skewness and Kurtosis of geoelectric signals

Targets: Earthquakes with $M_L \geq 5$

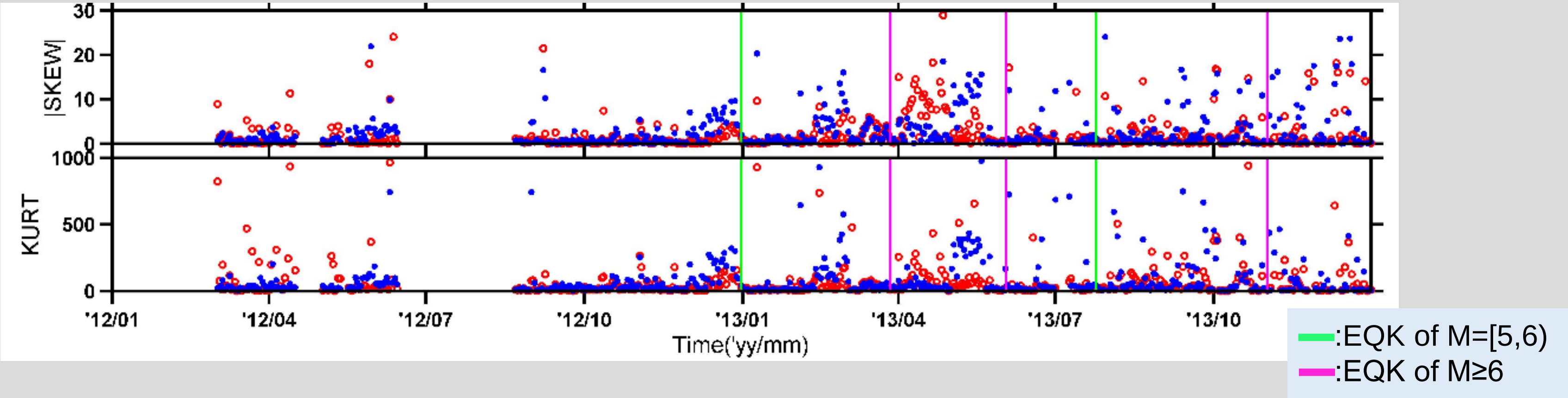

Full Dataset

Training phase | Forecasting phase

Onset Time

End Time: 2016/12/31

Step 2: Predictive Model

Model free parameters:

$$g = [M_c, R_c, A_{thr}, N_{thr}, T_{thr}, T_{obs}, T_{lead}, T_{pred}]$$

Definition of Target Earthquake (EQK):

1) Select magnitude-M_c-above EQK
2) Select source-to-station distances within R_c km.

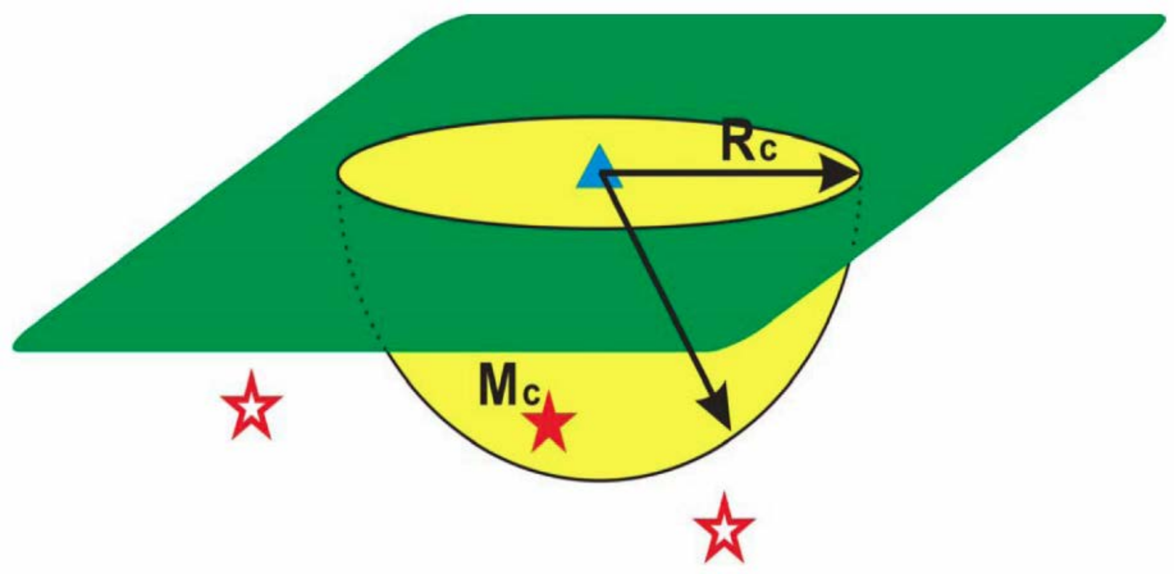

Definition of Time of Increased Probability (TIP):

1) **Median±A_{thr}*IQR:** Define an index as anomaly
2) **Anomalous index number (AIN) ≥ N_{thr}:** Label one day as an anomalous day
3) **Anomalous days ≥ T_{thr}** within T_{obs}: Alarm T_{pred} as TIP

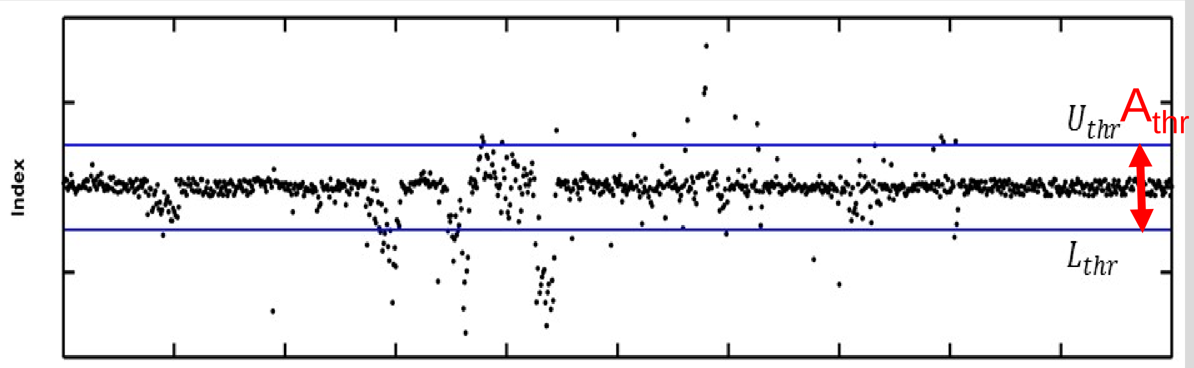

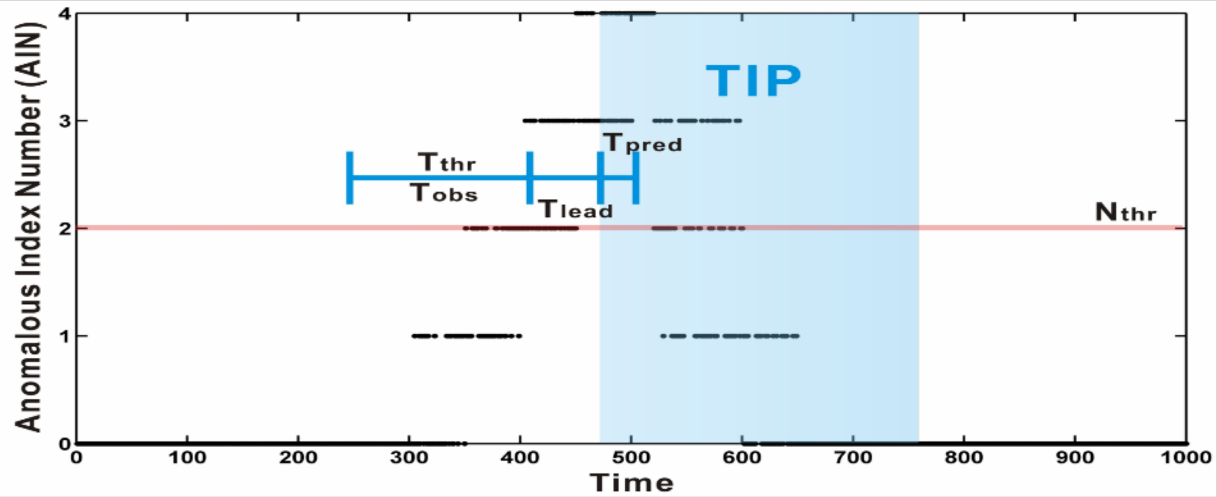

Step 3: Model Training

Model free parameters:

$$g = [M_c, R_c, A_{thr}, N_{thr}, T_{thr}, T_{obs}, T_{lead}, T_{pred}]$$

Parameter	Value
R_c	20-100 (km)
M_c	5
N_{thr}	1-4
A_{thr}	1-10
P_{thr}	0.1-0.5
T_{thr}	$[P_{thr} * T_{obs}]$ (day)
T_{obs}	5-100 (day)
T_{pred}	1 (day)
T_{lead}	0-100 (day)

1) Generate millions of parameter combinations g.
2) Estimate performance of each g by comparing the predicted time-space grids and the observed grids.

At a certain g,

$$Q(t|g) = \begin{cases} Q(t = t_i) = 1, \\ if \;\; M_{Li} \geq M_c \cap \|(x_i, y_i, z_i) - (x_{sta}, y_{sta}, 0)\| \leq R_c, i = 1 \;\; to \;\; N_{EQ} \\ Q = 0, otherwise \end{cases}$$

$$T_{TIP}(t|g) = \begin{cases} T_{TIP}(t = t_i + T_{lead} \;\; to \;\; t_i + T_{lead} + T_{pred}) = 1, if \;\; F_{SAT}(t_i) \geq T_{thr} \\ T_{TIP}(t = t_i + T_{lead} \;\; to \;\; t_i + T_{lead} + T_{pred}) = 0, \; if \;\; F_{SAT}(t_i) < T_{thr} \end{cases}$$

1: Alarm
0: No alarm

TIP	1	0	0	1	0	1	0	0	1….
EQK(Q)	1	0	0	0	1	0	0	0	1….

1: Earthquake
0: No earthquake

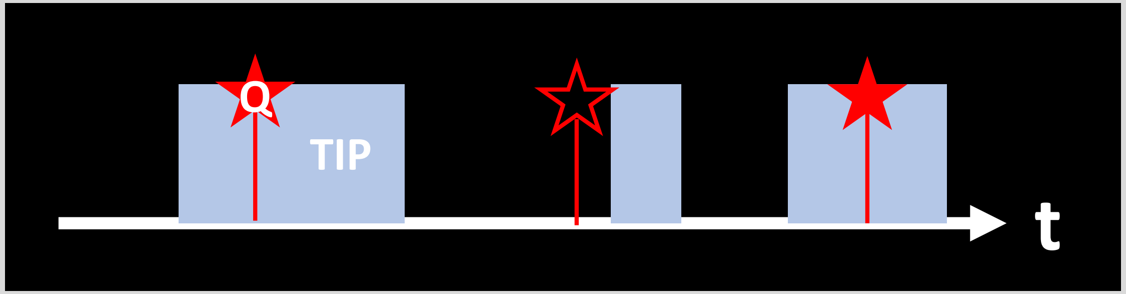

Molchan Diagram

Single station method

(1) Fraction of missing EQKs

$$n(\boldsymbol{g}) = \frac{\sum_t I(TIP(t|\boldsymbol{g})=0\ \&\ EQK(t|\boldsymbol{g})=1)}{\sum_t I(TIP(t|\boldsymbol{g})\geq 0\ \&\ EQK(t|\boldsymbol{g})=1)}$$

(2) Fraction of alarmed cells

$$\tau(\boldsymbol{g}) = \frac{\sum_t I(TIP(t|\boldsymbol{g})=1)}{\sum_t I(TIP(t|\boldsymbol{g})\geq 0)}$$

(3) Loss function of a parameter set

$$d(\boldsymbol{g}) = 1 - \tau(\boldsymbol{g}) - n(\boldsymbol{g})$$

The quantity d is the distance from a point to the random guess line.

1) d>0 means the performance is better than random.
2) d=0 means the performance is random.
3) d<0 means the performance is worse than random.

The model is significant when $d > d_{CB}^{max}$.

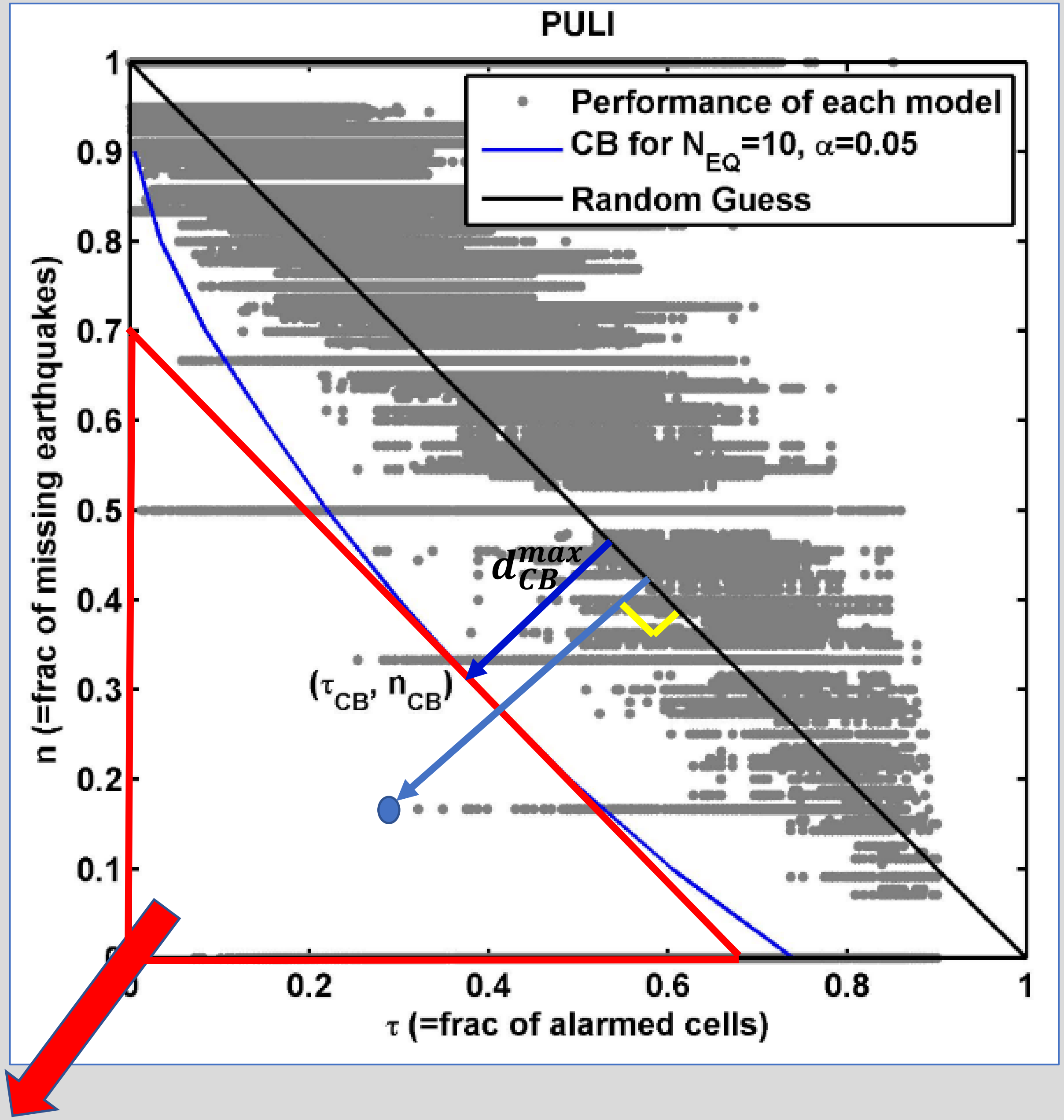

1) **Under the confidence bound:** **Parameters mean informative**
2) **Molchan diagram:** **Evaluate whether a prediction strategy is good**

Results (I): Choice of phase lengths

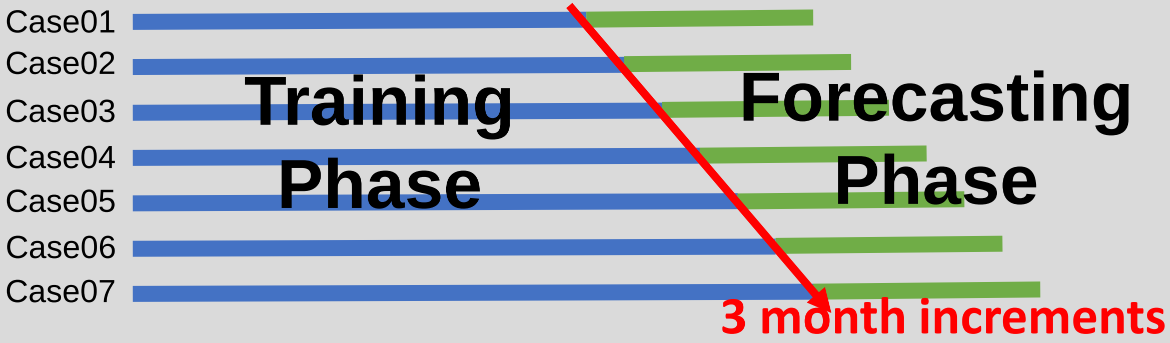

案例	訓練期(Trn)		預報期一季(Frc03)		預報期二季(Frc06)		預報期三季(Frc09)		預報期四季(Frc12)	
	時間	擬合程度(D)	時間	擬合程度(D)	時間	擬合程度(D)	時間	擬合程度(D)	時間	擬合程度(D)
01	測站啟用 - 2014/6/30	0.85± 0.24	2014/7/1- 2014/9/30	0.66± 0.14	2014/7/1- 2014/12/31	0.63± 0.15	2014/7/1- 2015/3/31	0.61± 0.18	2014/7/1- 2015/6/30	0.61± 0.18
02	測站啟用 - 2014/9/30	0.85± 0.15	2014/10/1- 2014/12/31	0.84± 0.17	2014/10/1- 2015/3/31	0.83± 0.17	2014/10/1- 2015/6/30	0.83± 0.17	2014/10/1- 2015/9/30	0.83± 0.17
03	測站啟用 - 2014/12/31	0.82± 0.14	2015/1/1- 2015/3/31	0.86± 0.10	2015/1/1- 2015/6/30	0.87± 0.10	2015/1/1- 2015/9/30	0.87± 0.10	2015/1/1- 2015/12/31	0.78± 0.22
04	測站啟用 - 2015/3/31	0.85± 0.03	2015/4/1- 2015/6/30	0.88± 0.03	2015/4/1- 2015/9/30	0.88± 0.03	2015/4/1- 2015/12/31	0.82± 0.17	2015/4/1- 2016/3/31	0.78± 0.22
05	測站啟用 - 2015/6/30	0.86± 0.04	2015/7/1- 2015/9/30	0.89± 0.03	2015/7/1- 2015/12/31	0.82± 0.18	2015/7/1- 2016/3/31	0.79± 0.28	2015/7/1- 2016/6/30	0.75± 0.32
06	測站啟用 - 2015/9/30	0.86± 0.03	2015/10/1- 2015/12/31	0.82± 0.18	2015/10/1- 2016/3/31	0.78± 0.22	2015/10/1- 2016/6/30	0.73± 0.27	2015/10/1- 2016/9/30	0.72± 0.27
07	測站啟用 - 2015/12/31	0.79± 0.18	2016/1/1- 2016/3/31	0.78± 0.18	2016/1/1 -2016/6/30	0.69± 0.21	2016/1/1- 2016/9/30	0.68± 0.21	2016/1/1- 2016/12/31	0.60± 0.27

$D(G_i)$ for i=1 to 10

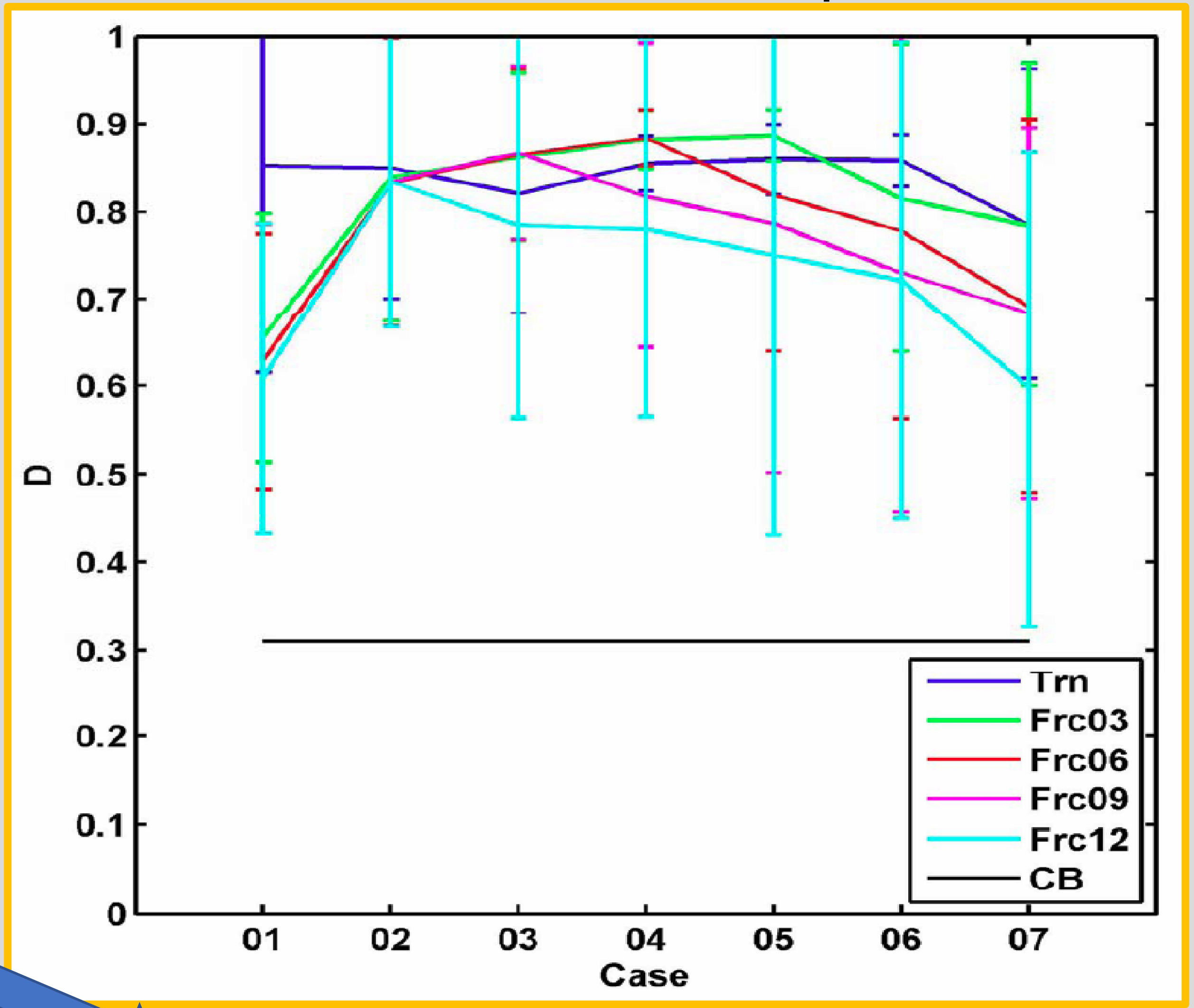

Optimal length:

1) **Training phase ~1000-1200 days**
2) **Forecasting phase ~90-180 days**

Results (II): Choice of frequency band

High-pass filter:

$$|H(f)| = \begin{cases} 1, |f| < f_c \\ 0, |f| > f_c \end{cases}$$

Low-pass filter:

$$|H(f)| = \begin{cases} 0, |f| < f_c \\ 1, |f| > f_c \end{cases}$$

$f_c = 10^{(-4:0.25:-0.5)}$ **Hz**

Periods:
1) Training: Onset-2015/3/31
2) Forecast: 2015/4/1-2015/6/30

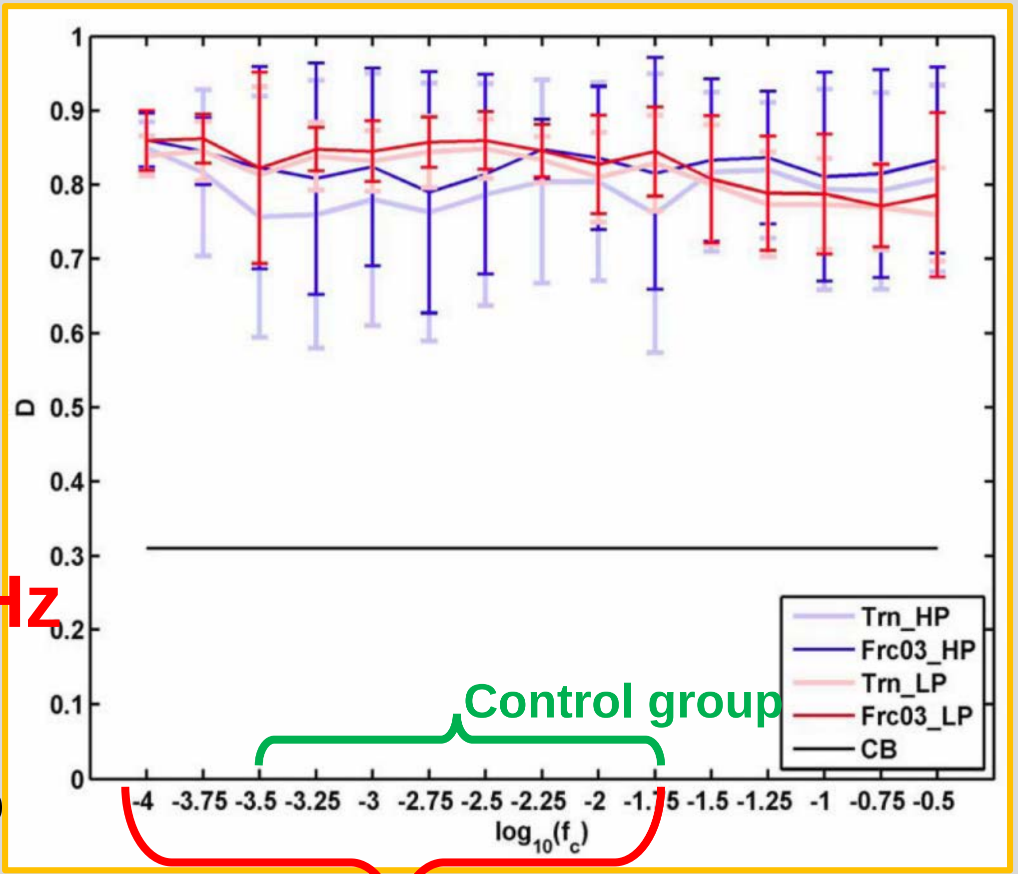

Optimal band

Band-pass filter:

$$|H(f)| = \begin{cases} 1, f_1 < |f| < f_2 \\ 0, otherwise \end{cases}$$

(1) $10^{-4.0} \leq f \leq 10^{-1.75}$ Hz

(T=~1min-~3hr, optimal band)

(2) $10^{-3.5} \leq f \leq 10^{-1.75}$ Hz

(T=~1min-~1hr, for control group)

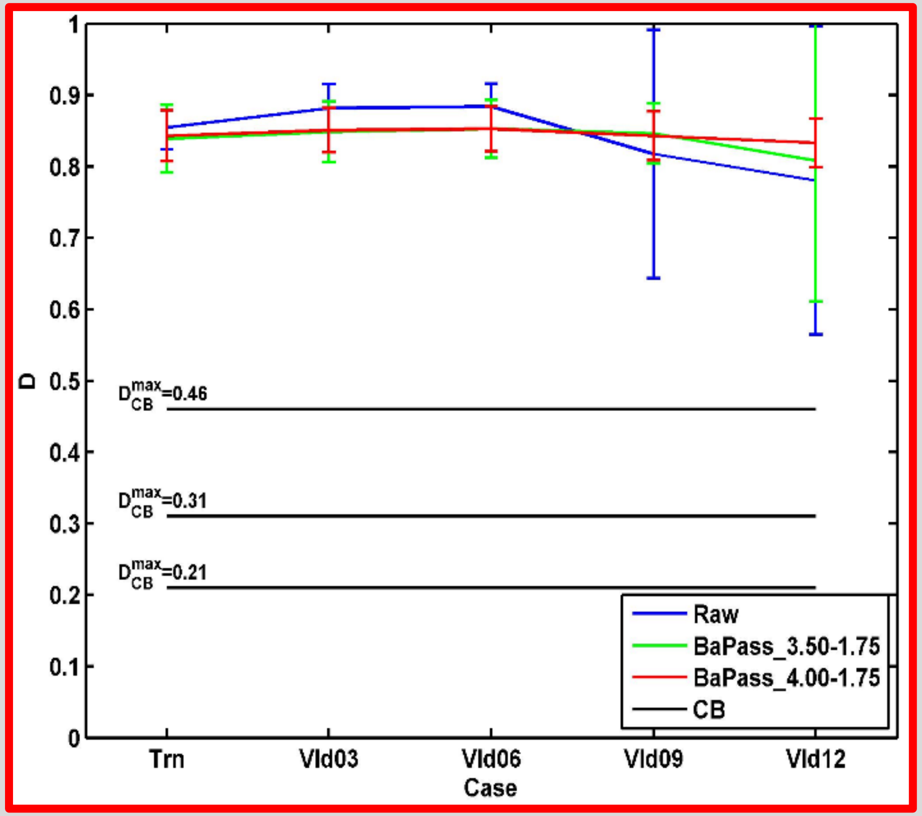

Earthquake-related signal:

1) **High S/N ratio**
2) **Constrain the prediction model stably**

Results (III): Precursor-based Earthquake Probability Forecasts

$$P(x,y,t) = \frac{1}{N_{top}} \sum_{i=1}^{N_{top}} v(G_i) \cdot T_{TIP}(x,y,t|G_i),$$

Construct earthquake-forecasting probability P(x,y,t) using True Positive Rate (TPR, v=1-n) multiplied by TIP.

Raw data

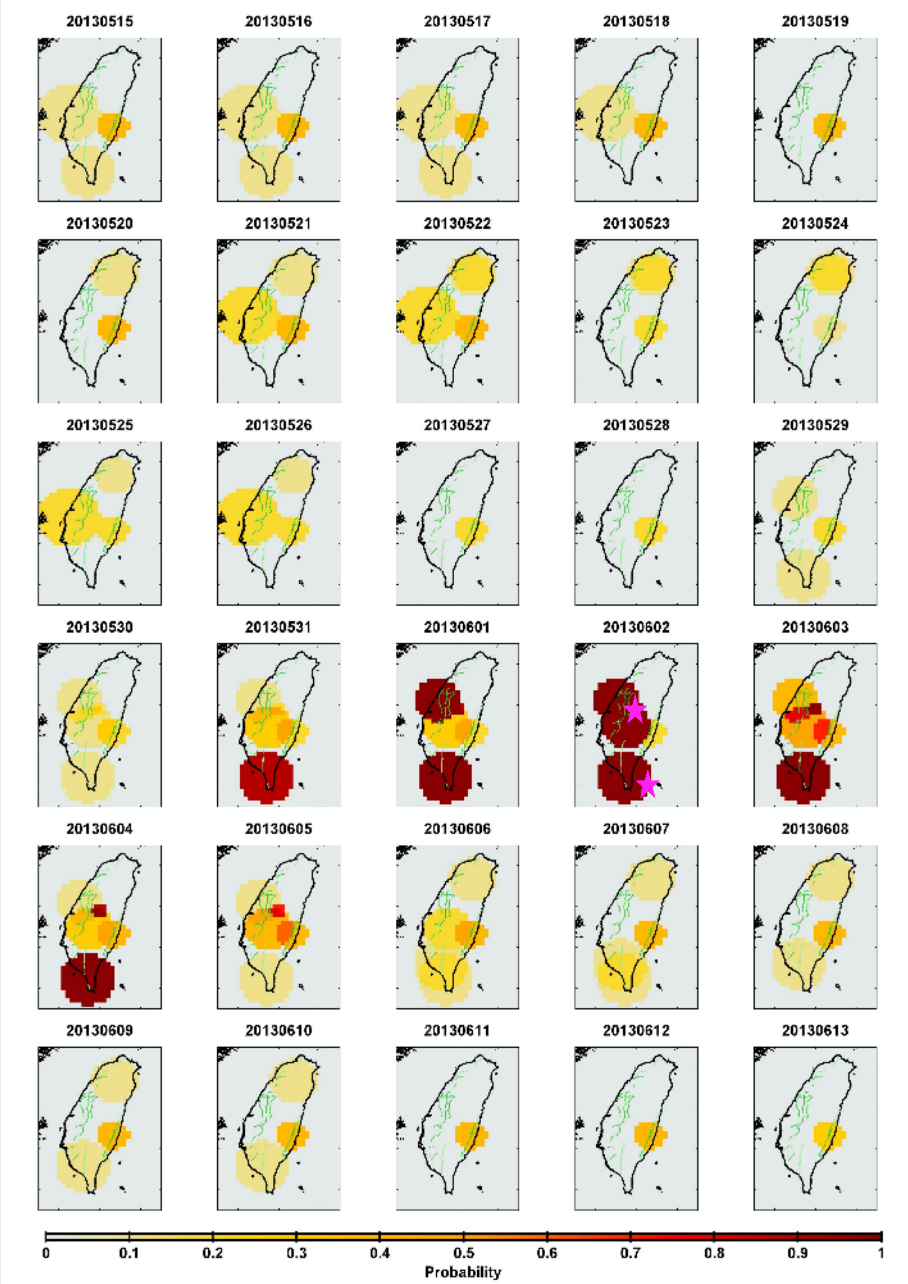

Bandpass filtered data $10^{-4.0} \leq f \leq 10^{-1.75}$ Hz

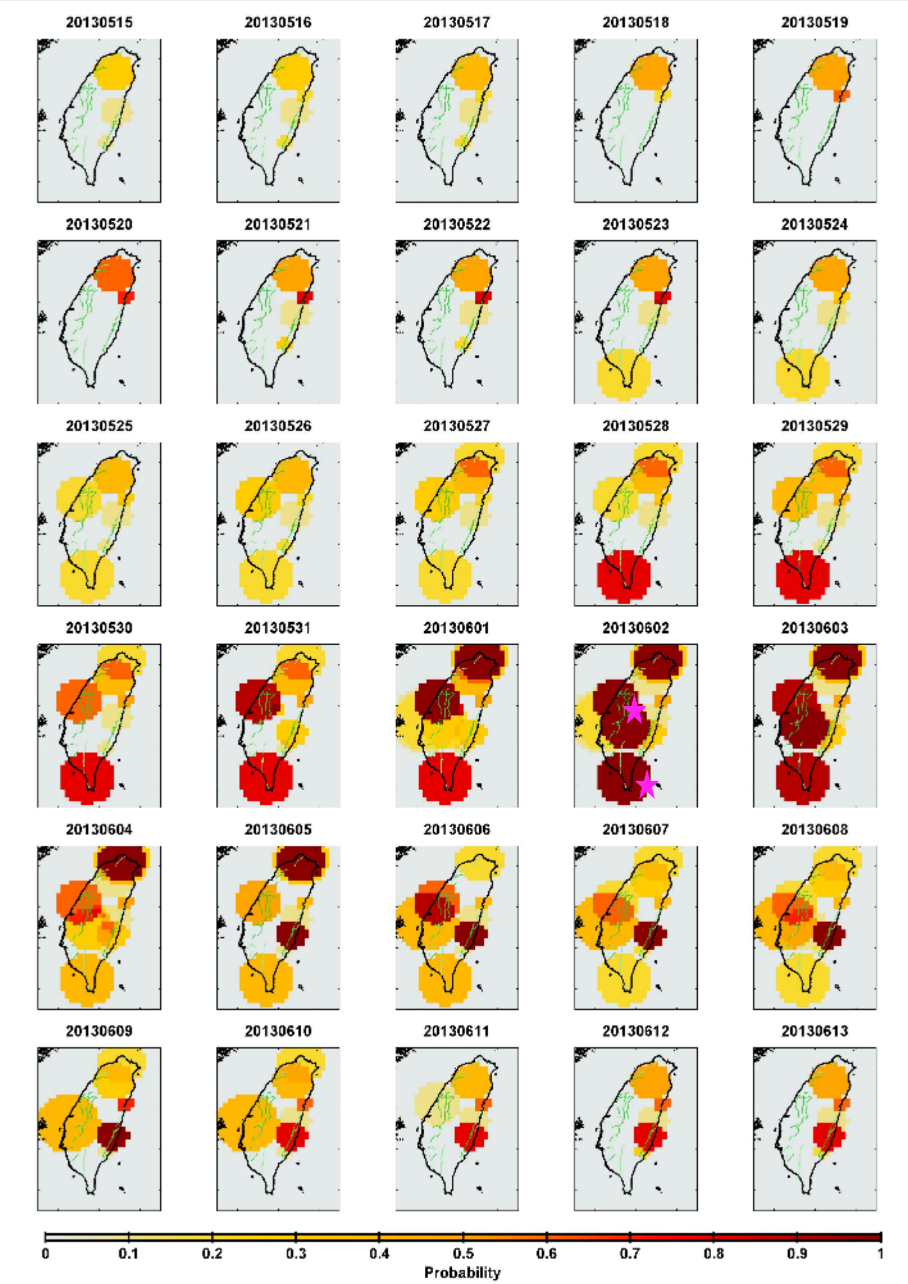

Summary of GEMSTIP Analysis

- **Quantitative examination:** Testing relationships between geoelectric field statistics and earthquakes.

- Significance tests: Seismo-electric relationship **objectively exists**.

- Optimal frequency band **($10^{-4.0} \leq f \leq 10^{-1.75}$ Hz, T=~1min-~3hr):** Earthquake-related signals with high S/N ratio

Observation (III): Pre-earthquake anomalies at Kakioka, Japan

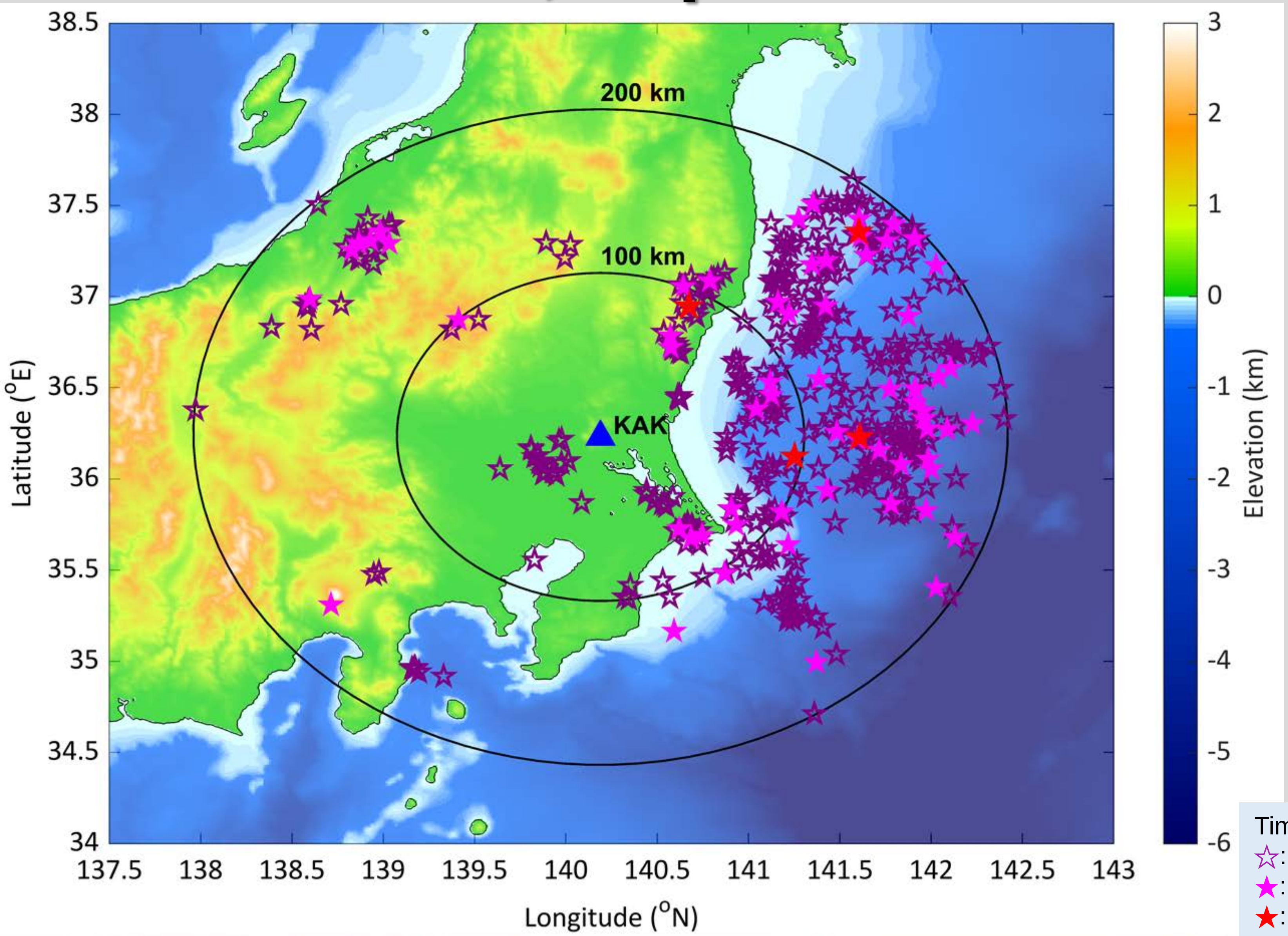

Time: 19930101-20181231
☆:EQK of M=[5,6)
★:EQK of M=[6,7)
★:EQK of M≥7

Purpose:

(1) To confirm the GEMSTIP algorithm can be valid for other regions
(2) To improve the way of selecting optimal model parameters

Data:

- **Kakioka station (KAK):**
  - location: 36.23°N, 140.1°E
  - self-potential data
  - sampling rate: 1 point per minute
  - from 1993 to 2018
- **Earthquake:**
  - 488 $M_L \geq 5$ EQKs
  - from 1993 to 2018

Geoelectric time series

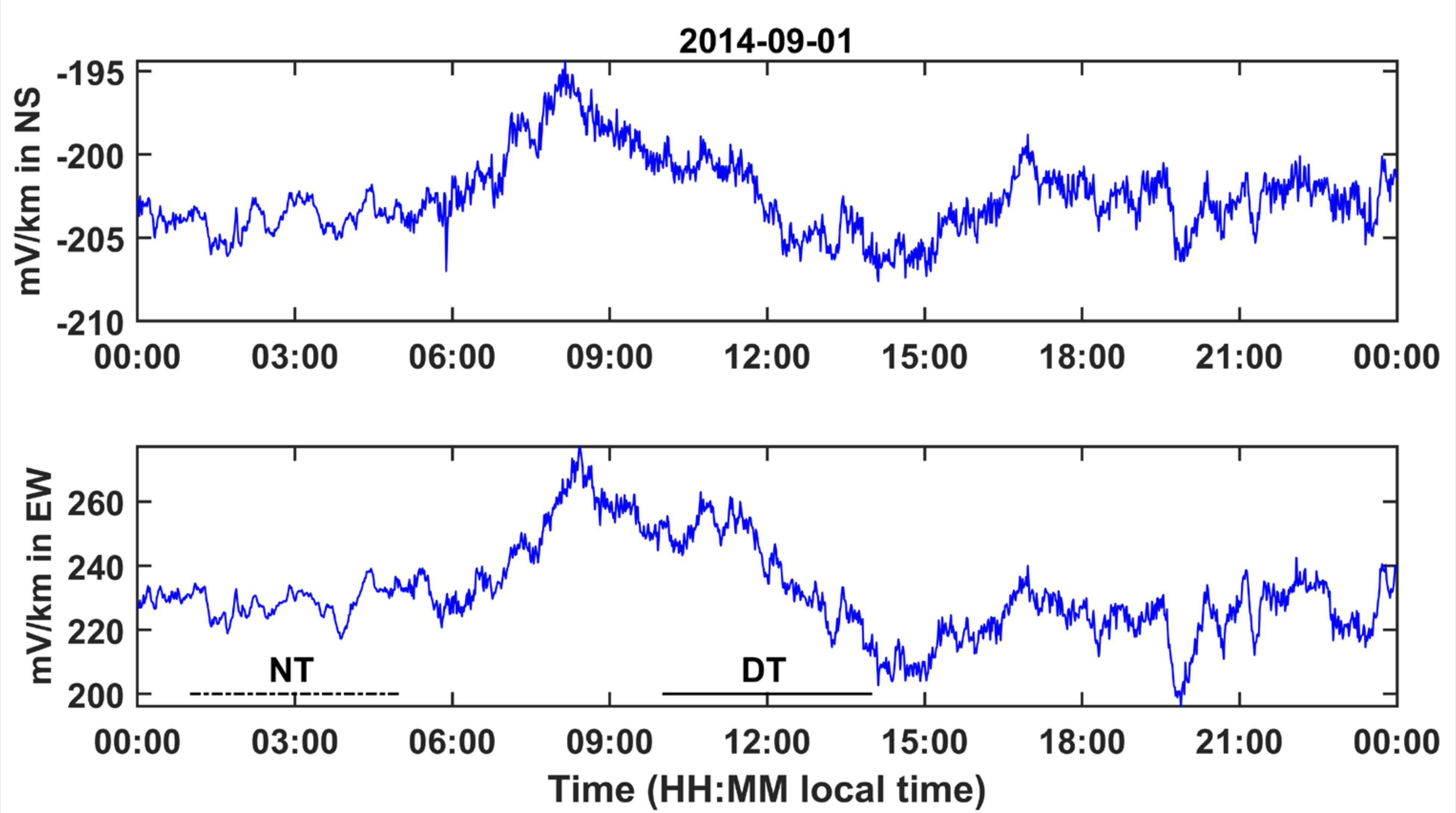

The nighttime data has less noises that the daytime data.
In this study we calculate variance, skewness, and kurtosis by using nighttime data.

Variance-Skewness-Kurtosis Time Series

Time series of V, S, K
with their thresholds:
MD ± Athr*IQR

Threshold:
Window length = 1000 days
A_{thr} = 2

EQ selection:
M_{thr} = 5
R_{thr} = 100 km

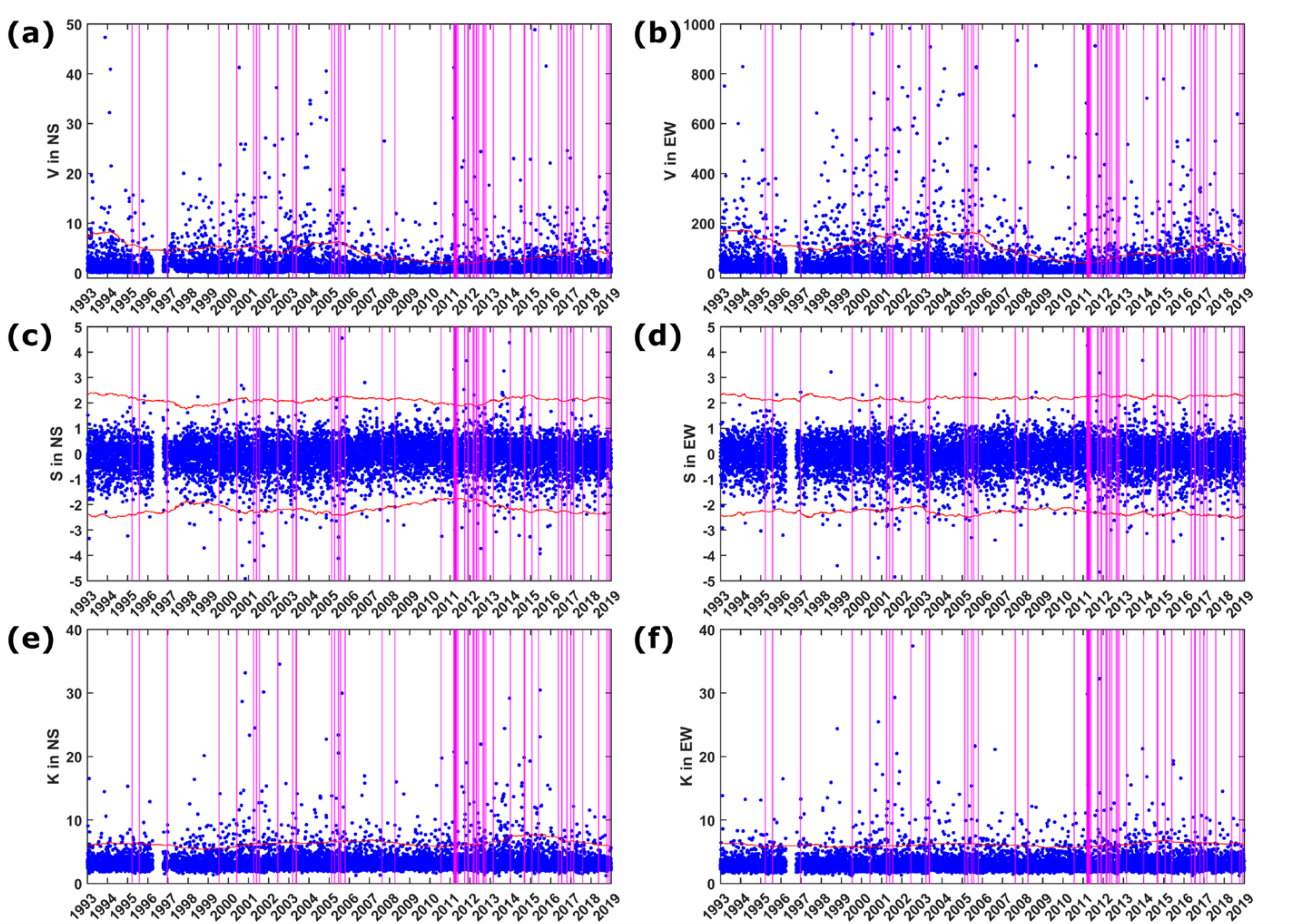

Anomaly Index Number (AIN) & Superposed Epoch Analysis (SEA)

Time series of AIN for V, S, and K
Thresholds: MD ± Athr*IQR
A_{thr} = 1, 2, and 3

EQ selection:
M_{thr} = 6
R_{thr} = 100 km

SEA finds that anomalies are highly likely to occur **6 and 58 days** before strong earthquakes

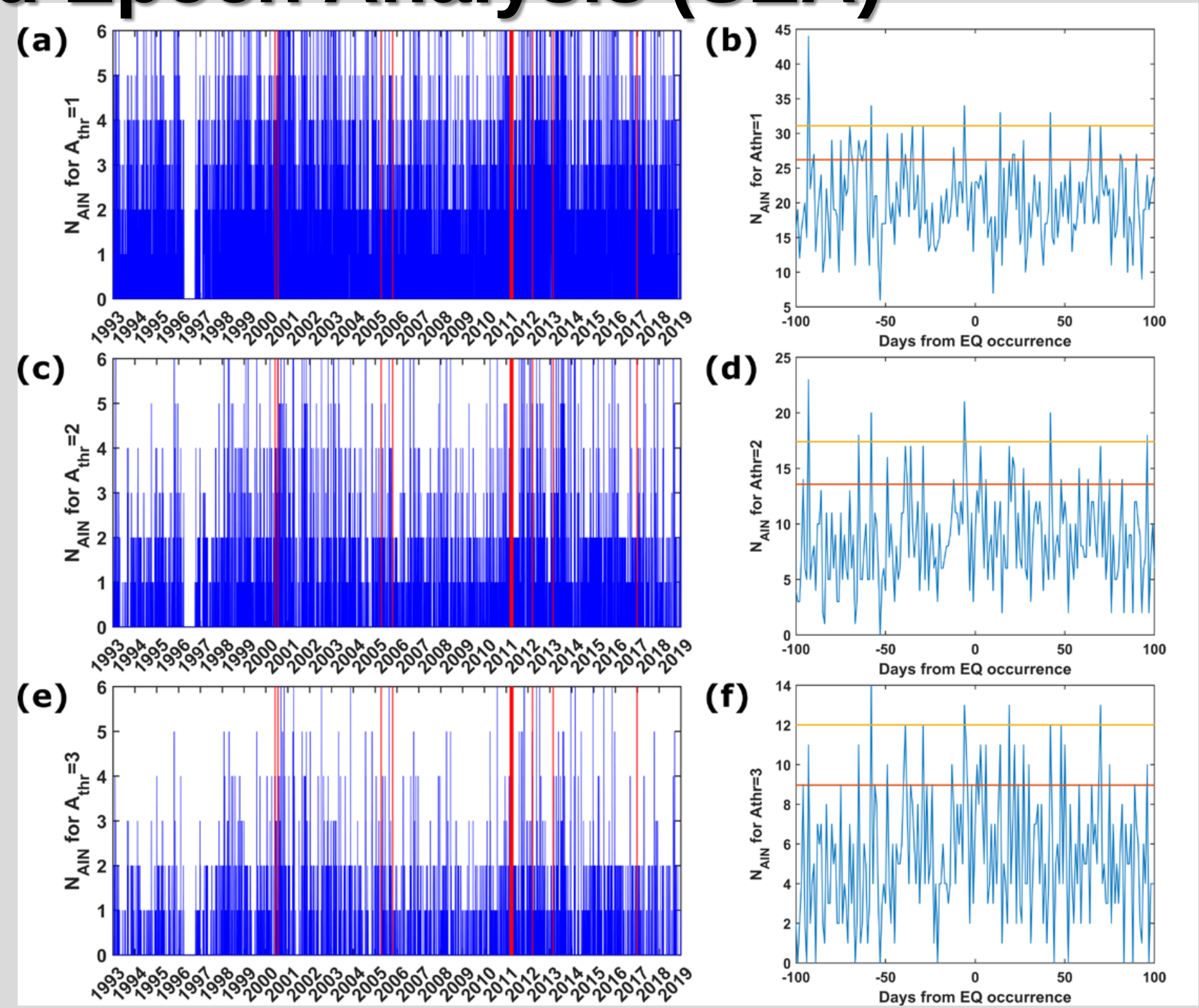

Predictive Model

Model parameter:

$$\boldsymbol{g} = [M_{thr}, R_{thr}, A_{thr}, P_{thr}, T_{obs}, T_{lead}, T_{pred}]$$

Target events:

$$F_{obs}(t|\boldsymbol{g}) = B[(r_i \le R_{thr}) \cdot (m_i \ge M_{thr}) \cdot (t = t_i)], t \in [t_s, t_e]$$

Time of increased probability (TIP):

$$\theta_u(t; y) = Median(y_i) + A_{thr} * IQR(y_i), i \in [t - \Delta t, t]$$

$$\theta_l(t; y) = Median(y_i) - A_{thr} * IQR(y_i), i \in [t - \Delta t, t]$$

$$N_{AIN}(t|\boldsymbol{g}) = \sum_y B\left[\left(y(t) > \theta_u(t; y)\right) + \left(y(t) < \theta_l(t; y)\right)\right]$$

$$\bar{N}_{AIN,T_{obs}}(t|\boldsymbol{g}) = \frac{\sum_{i=t-T_{obs}+1}^{t} N_{AIN}(i|\boldsymbol{g})}{T_{obs}}$$

$$R_{AIN,T_{obs}}(t|\boldsymbol{g}) = \frac{\bar{N}_{AIN,T_{obs}}(t|\boldsymbol{g})}{\max_{t \in [t_s, t_e]} \bar{N}_{AIN,T_{obs}}(t|\boldsymbol{g})}$$

$$F_{at}(t|\boldsymbol{g}) = B\left[R_{AIN,T_{obs}}(t|\boldsymbol{g}) \ge P_{thr}\right]$$

$$F_{tip}(t|\boldsymbol{g}) = B\left[\left(t = t_i|_{F_{at}=1} + T_{lead} + 1\right) + \left(t = t_i|_{F_{at}=1} + T_{lead} + 2\right) + \cdots + \left(t = t_i|_{F_{at}=1} + T_{lead} + T_{pred}\right)\right], t \in [t_s, t_e]$$

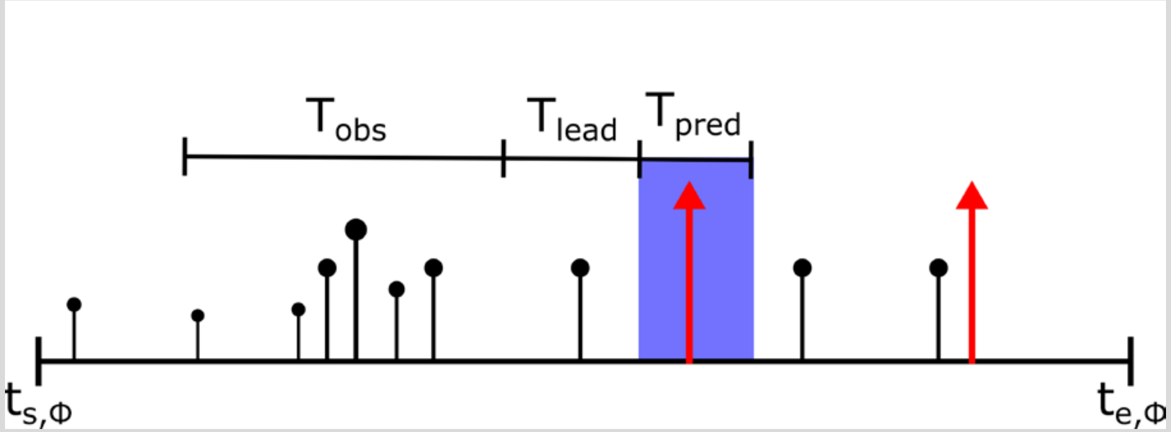

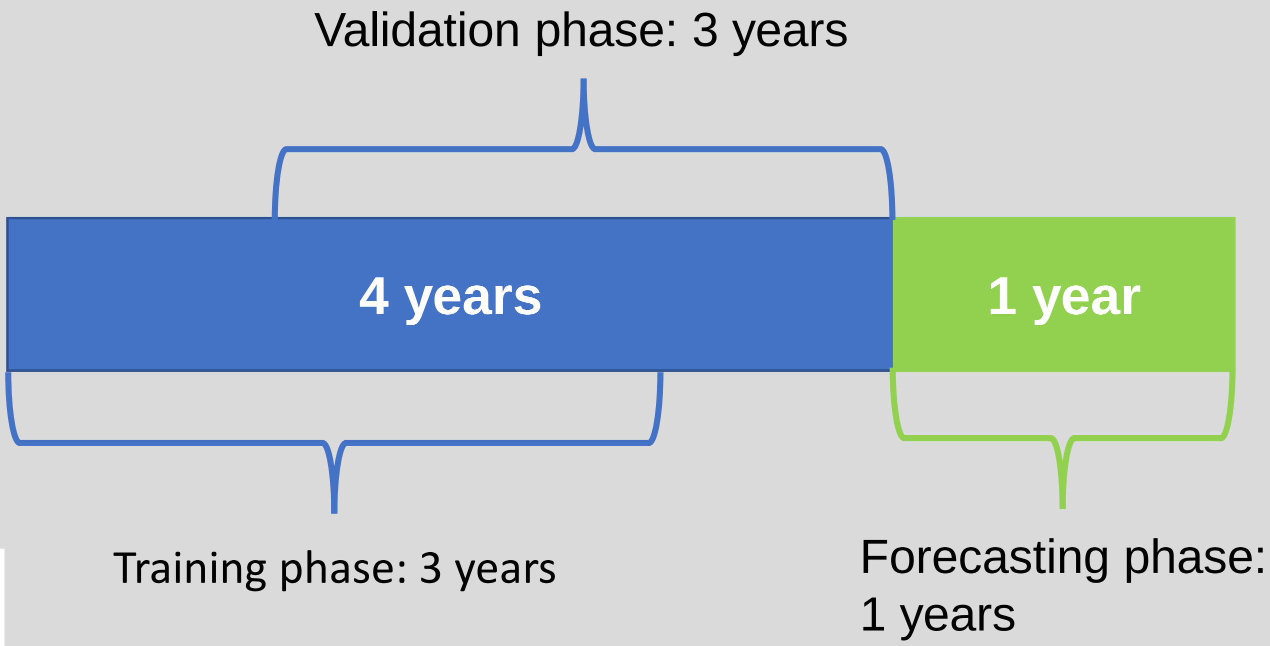

Performance Score

[Keilis-Borok et al., 2009]

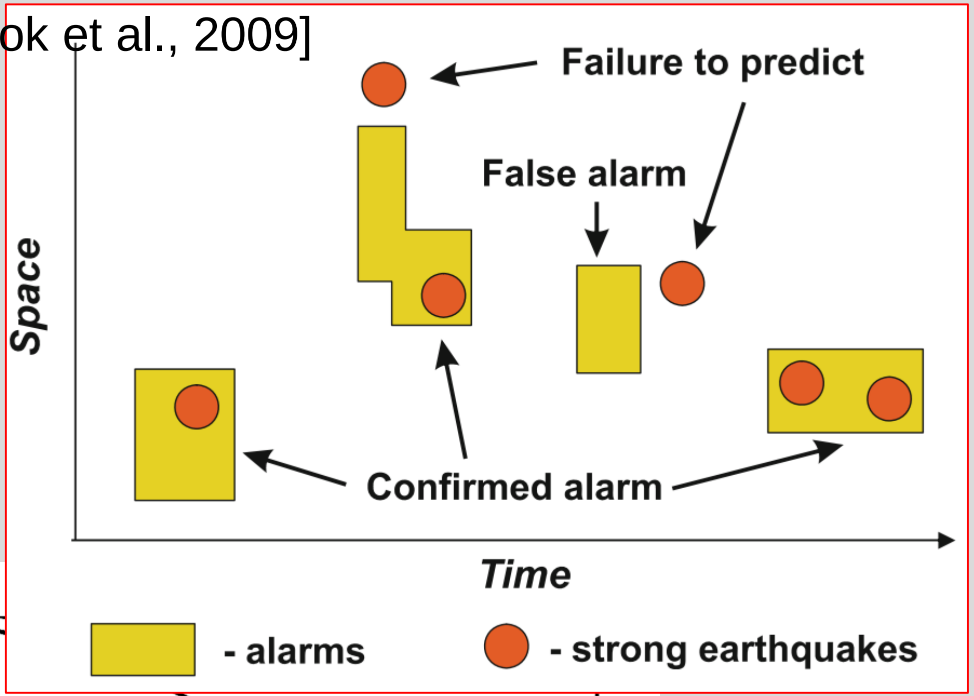

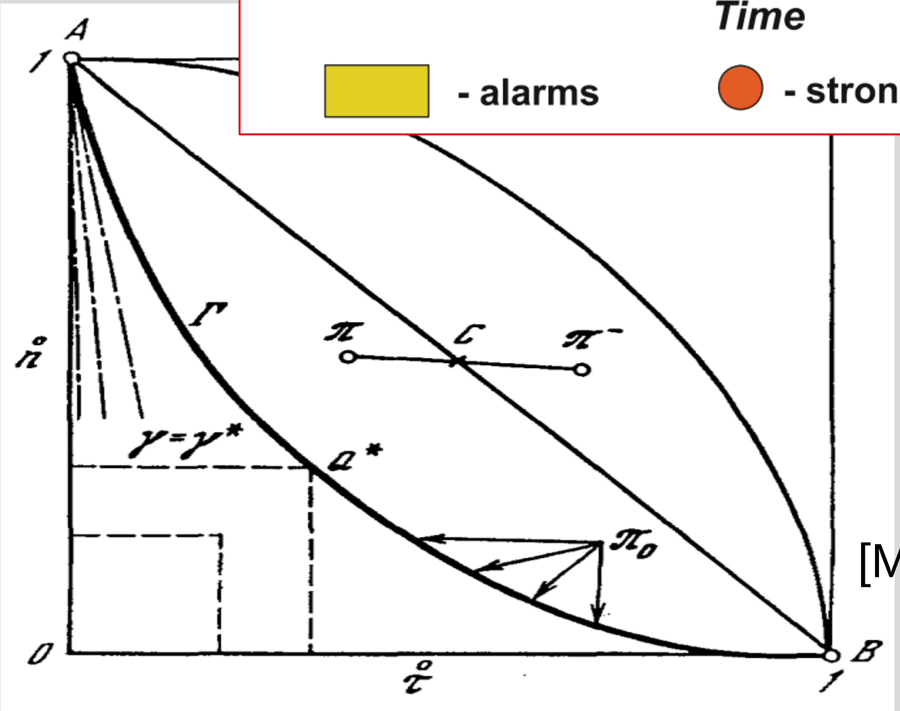

[Molchan, 1997]

Ratio of alarmed cells

$$\tau(\boldsymbol{g}) = \frac{\sum_t F_{tip}(t|\boldsymbol{g})}{\sum_t B[F_{tip}(t|\boldsymbol{g}) \geq 0]}$$

Ratio of missed events

$$n(\boldsymbol{g}) = \frac{\sum_t B[(F_{tip}(t|\boldsymbol{g})=0)\cdot(F_{obs}(t|\boldsymbol{g})=1)]}{\sum_t B[(F_{tip}(t|\boldsymbol{g})\geq 0)\cdot(F_{obs}(t|\boldsymbol{g})=1)]}$$

Loss function:

$$d(\boldsymbol{g}) = 1 - \tau(\boldsymbol{g}) - n(\boldsymbol{g})$$

Maximum loss function

$$D = \max_{i=1\ to\ N_{OM}} \{d(\hat{\boldsymbol{g}}_i; frc)\}$$

Maximum probability gain

$$PG = \max_{i=1\ to\ N_{OM}} \left\{\frac{1-n(\hat{\boldsymbol{g}}_i; frc)}{\tau(\hat{\boldsymbol{g}}_i; frc)}\right\}$$

Ratio of numbers of positive to negative models

$$\rho = \frac{\sum_{i=1}^{N_{OM}} B[d(\hat{\boldsymbol{g}}_i; frc) > 1]}{\sum_{i=1}^{N_{OM}} B[d(\hat{\boldsymbol{g}}_i; frc) < 1]}$$

Forecasting Performance

Case	Training phase	Validation phase	Forecasting phase	PG	D	ρ
1	1993/1/1-1995/12/31	1994/1/1-1996/12/31	1997/1/1-1997/12/31	2.94	0.66	1.3
2	1994/1/1-1996/12/31	1995/1/1-1997/12/31	1998/1/1-1998/12/31	1.96	0.39	1.48
3	1995/1/1-1997/12/31	1996/1/1-1998/12/31	1999/1/1-1999/12/31	1.72	0.42	1.14
4	1996/1/1-1998/12/31	1997/1/1-1999/12/31	2000/1/1-2000/12/31	1.69	0.41	0.72
5	1997/1/1-1999/12/31	1998/1/1-2000/12/31	2001/1/1-2001/12/31	11.41	0.85	1.91
6	1998/1/1-2000/12/31	1999/1/1-2001/12/31	2002/1/1-2002/12/31	2.06	0.48	0.83
7	1999/1/1-2001/12/31	2000/1/1-2002/12/31	2003/1/1-2003/12/31	1.69	0.34	1.84
8	2000/1/1-2002/12/31	2001/1/1-2003/12/31	2004/1/1-2004/12/31	3.08	0.59	1.66
9	2001/1/1-2003/12/31	2002/1/1-2004/12/31	2005/1/1-2005/12/31	3.43	0.49	1.93
10	2002/1/1-2004/12/31	2003/1/1-2005/12/31	2006/1/1-2006/12/31	3.61	0.72	0.1
11	2003/1/1-2005/12/31	2004/1/1-2006/12/31	2007/1/1-2007/12/31	3.07	0.67	2
12	2004/1/1-2006/12/31	2005/1/1-2007/12/31	2008/1/1-2008/12/31	4.52	0.52	1.57
13	2005/1/1-2007/12/31	2006/1/1-2008/12/31	2009/1/1-2009/12/31	2.5	0.35	1.28
14	2006/1/1-2008/12/31	2007/1/1-2009/12/31	2010/1/1-2010/12/31	15.21	0.93	0.83
15	2007/1/1-2009/12/31	2008/1/1-2010/12/31	2011/1/1-2011/12/31	1.71	0.41	1.49
16	2008/1/1-2010/12/31	2009/1/1-2011/12/31	2012/1/1-2012/12/31	1.45	0.28	0.88
17	2009/1/1-2011/12/31	2010/1/1-2012/12/31	2013/1/1-2013/12/31	1.26	0.14	0.08
18	2010/1/1-2012/12/31	2011/1/1-2013/12/31	2014/1/1-2014/12/31	6.76	0.85	1.42
19	2011/1/1-2013/12/31	2012/1/1-2014/12/31	2015/1/1-2015/12/31	3.38	0.55	4.08
20	2012/1/1-2014/12/31	2013/1/1-2015/12/31	2016/1/1-2016/12/31	1.51	0.22	0.12
21	2013/1/1-2015/12/31	2014/1/1-2016/12/31	2017/1/1-2017/12/31	1.4	0.14	0.14

Average D = 0.49
Average PG = 3.68
ρ>1 case: 14 out of 22

Forecasting Probability & Optimal model parameters

Positive case

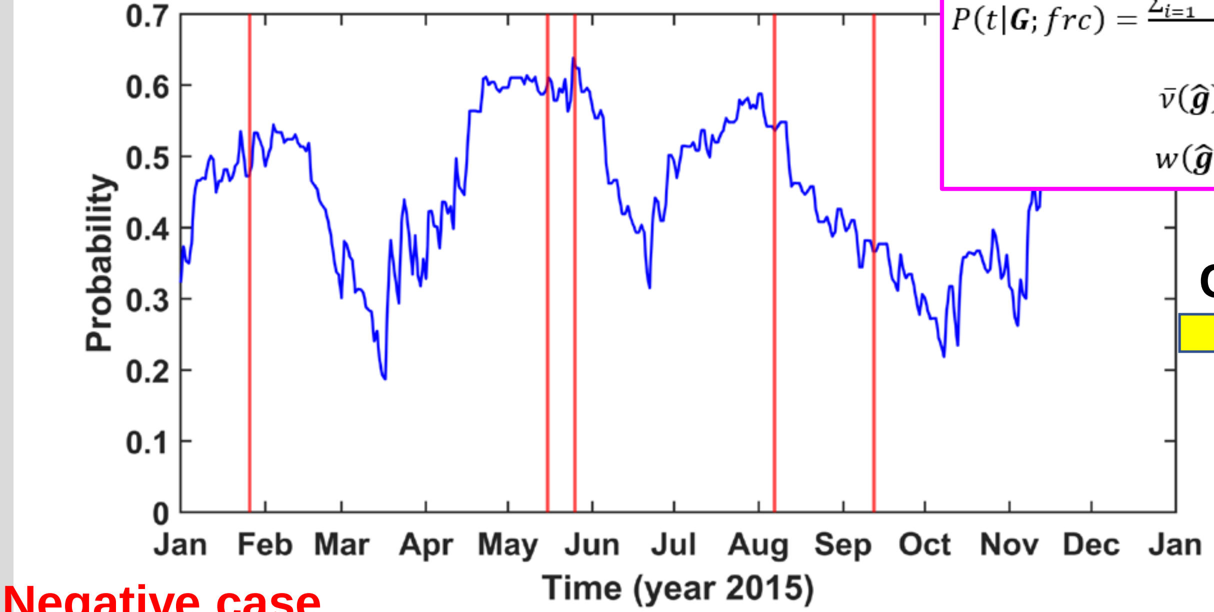

$$P(t|\boldsymbol{G};frc) = \frac{\sum_{i=1}^{N_{OM}} F_{tip}(t|\widehat{\boldsymbol{g}}_i;frc)\cdot\bar{v}(\widehat{g}_i)\cdot w(\widehat{g}_i)}{\sum_{i=1}^{N_{OM}} w(\widehat{g}_i)}$$

$$\bar{v}(\widehat{\boldsymbol{g}}) = 1 - \bar{n}(\widehat{\boldsymbol{g}})$$

$$w(\widehat{\boldsymbol{g}}) = 1 - \bar{\tau}(\widehat{\boldsymbol{g}})$$

Case 19

Negative case

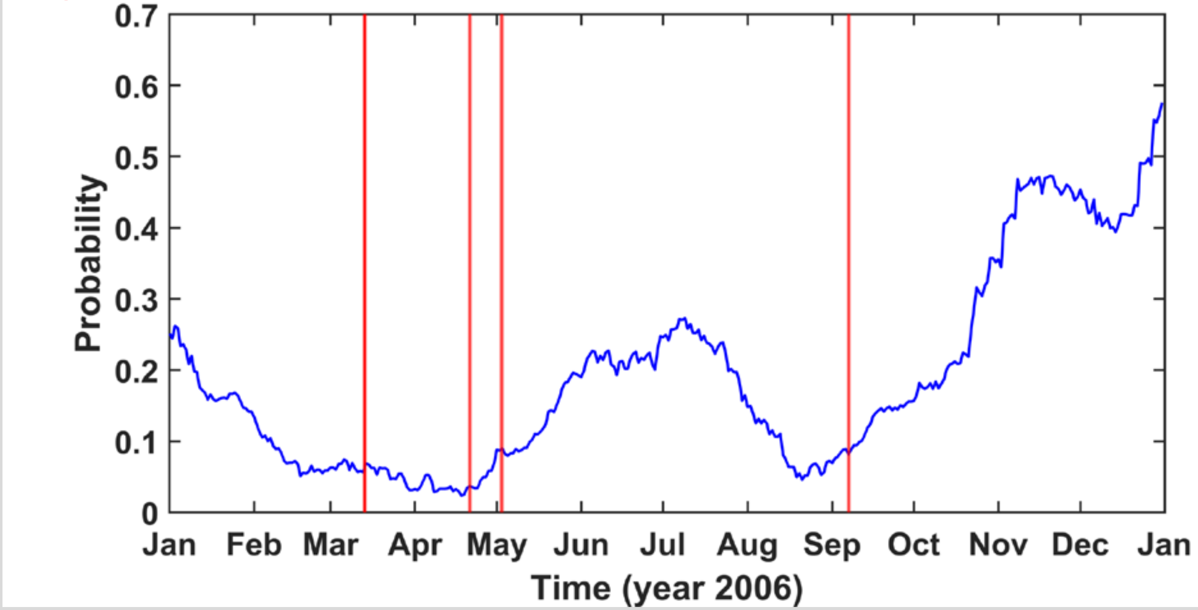

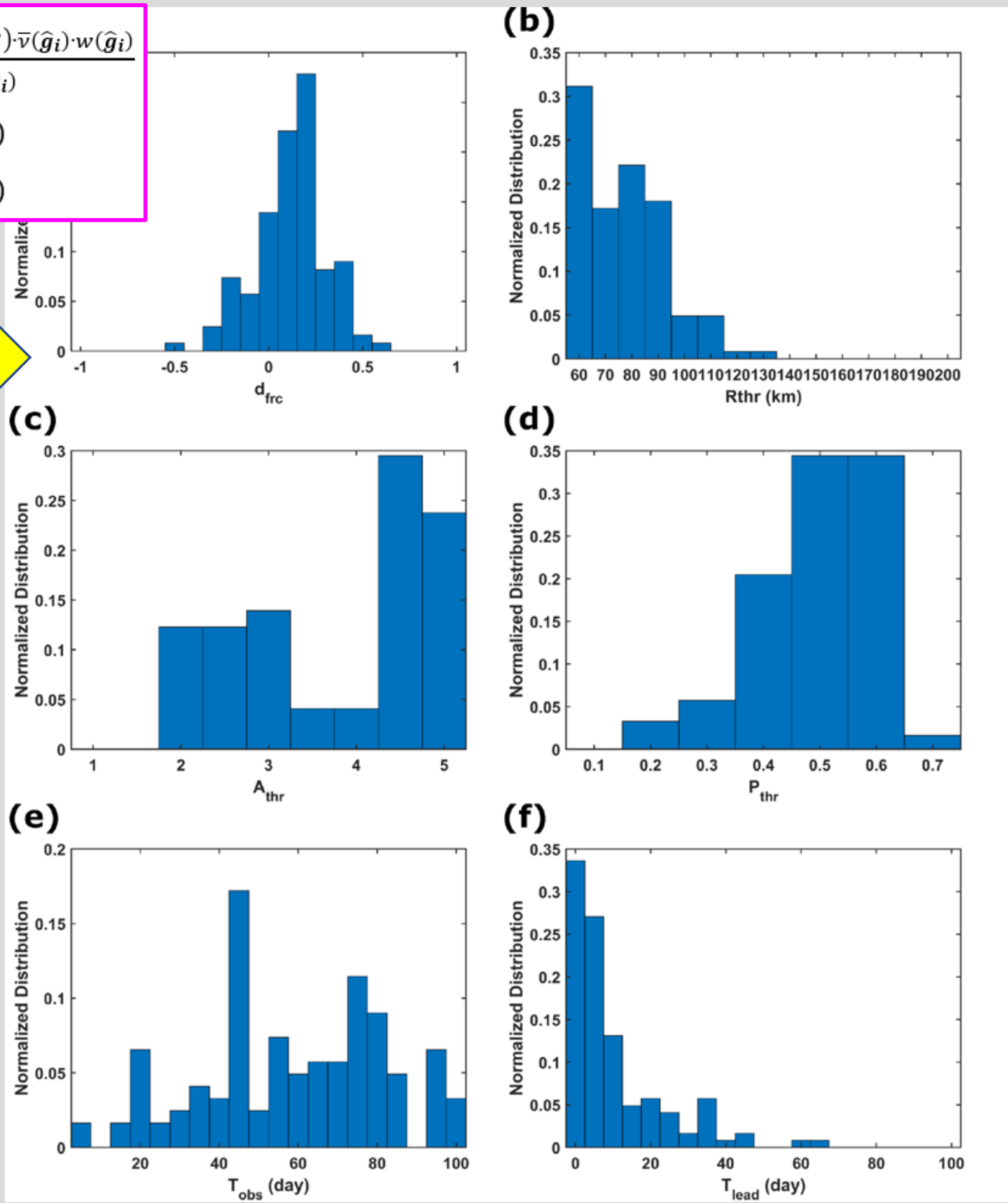

Summary of Pre-seismic Anomalies

- Pre-seismic anomalies for self-potential variance, skewness, and kurtosis are investigated and verified at Kakioka, Japan.
- The predictive model parameter can be optimized and selected through model scores of the training phase and validation phase.
- The optimal model parameters can be well-performed. There are 14 positive cases out of 22 cases through 26-year long-term analysis.

Conclusions

- **Seismo-electric model (Chen-Ouillon-Sornette model)**
  1) explains transient EM anomalies before large EQKs, such as skewness and kurtosis anomalies, PSD power-law exponent transitions.
  2) explains cases of no prominent EM anomalies before large EQKs

- **For long-term average behavior, the self-potential signals with f = 0.006-1 Hz are correlated with mechanics in the crust, but less correlated with human-made noises.**

Conclusions

- GEMSTIP algorithm
  1) provides a quantitative examination of relationships between geoelectric field statistics and earthquakes.
  2) provides significance tests for seismo-electric relationship objectively existing.
  3) determines $10^{-4.0} <= f <= 10^{-1.75}$ Hz (T=~1min-~3hr) as the frequency bands with high S/N ratio.
- GEMSTIP algorithm is valid for the Taiwan and Japan regions. This means the geoelectric data distributions universally deviate from normal distributions before earthquakes.

Future Studies

- ➢ For physical perspectives, we need to further study the coupling between mechanics and electromagnetics in the crust
  - Geomagnetic and geoelectric data versus strain rates
  - Geomagnetic and geoelectric data versus seismic velocity ratio
  - Geomagnetic and geoelectric data versus attenuation ratio (Q)
- ➢ For model simulations, we have to consider the foreshock and aftershock effects into the stick-slip models.

Future Studies

- For statistical perspectives, we should test other precursory indices proposed by earlier studies, such as natural time analysis, principle component analysis, and network topology analysis.
- The logic of our future work:
  - The multi-phenomena nature of earthquake precursors
  - A unifying theory in terms of stress activation of mobile electric charges
  - Continuous multi-observational, multi-dimensional monitoring
  - Multi-dimensional analyses and synthesis of precursors
  - A decision-making process towards operational and practical forecasts

Thank you for listening!